

Moduli Spaces of Pentagonal Subdivision Tilings

Jinjin Liang, Erxiao Wang*, Zhejiang Normal University
Min Yan†, Hong Kong University of Science and Technology

Abstract

Pentagonal subdivision gives three families of edge-to-edge tilings of the sphere by congruent pentagons. Each family forms a two dimensional moduli space. We describe these moduli spaces in detail.

2010 Mathematics Subject Classification: Primary 52C20, 05B45.

Keywords: Spherical tiling, Moduli space, Pentagon, Subdivision.

Sommerville [9] started the classification of edge-to-edge tilings of the sphere by congruent triangles in 1924, and Ueno and Agaoka [10] completed the classification in 2002. In [1, 2, 3, 5, 4, 6, 7, 8, 11, 12], we completely classified edge-to-edge tilings of the sphere by congruent polygons. The tilings are the Platonic type, the earth map type, and several quadrilateral tilings of the sporadic type.

The tilings allow up to two free parameters. Quite a number of tilings allow one free parameter, and the ranges of the parameters are well understood. There are five tilings allowing two free parameters: The tetrahedron P_4 , the first quadrilateral earth map tiling $E_{\square}1$, and the three pentagonal subdivisions PP_4, PP_8, PP_{20} of the Platonic solids. The moduli space of the tiling P_4 is all the spherical triangles such that the sum of three angles is 2π .

*Corresponding author (wang.eric@zjnu.edu.cn). Research was supported by National Natural Science Foundation of China NSFC-RGC 12361161603 and Key Projects of Zhejiang Natural Science Foundation LZ22A010003.

†Research was supported by NSFC-RGC Joint Research Scheme N-HKUST607/23 and Hong Kong RGC General Research Fund 16305920.

The moduli space of the tiling $E_{\square}1$ is described in [4, Figure 51] and [7, Figure 13]. The moduli spaces of the pentagonal subdivisions PP_4, PP_8, PP_{20} are more complicated, and are discussed in detail in this paper.

The pentagonal subdivision divides (more precisely, replaces) each triangular face F of the regular tetrahedron P_4 , octahedron P_8 or icosahedron P_{20} into three congruent pentagons with edge lengths a, a, b, b, c . See the subdivision scheme in the first of Figure 1. Actually we do not keep the edges of F straight. The second of Figure 1 is the perspective picture of the stereographic projection of the pentagonal subdivision of a face F of the tetrahedron, while Figure 2 gives real 3D pictures of three pentagonal subdivision tilings. The angles of the regular triangle F are $\frac{2}{n}\pi$. Here and throughout the paper, $n = 3, 4, 5$ is reserved for the tetrahedron, octahedron, icosahedron.

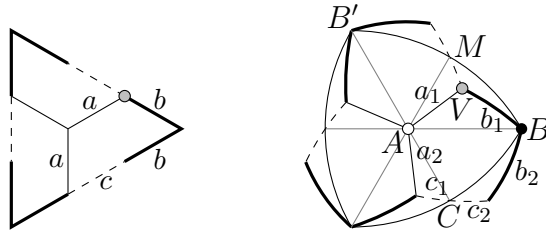


Figure 1: Pentagonal subdivision of a regular triangle.

In the second of Figure 1, A, B, C are the center of F , a vertex of F , and the middle point of an edge of F . Moreover, let B' and M be the rotations of B and C around the center A by $\frac{2}{3}\pi$. Then M is the middle point of BB' .

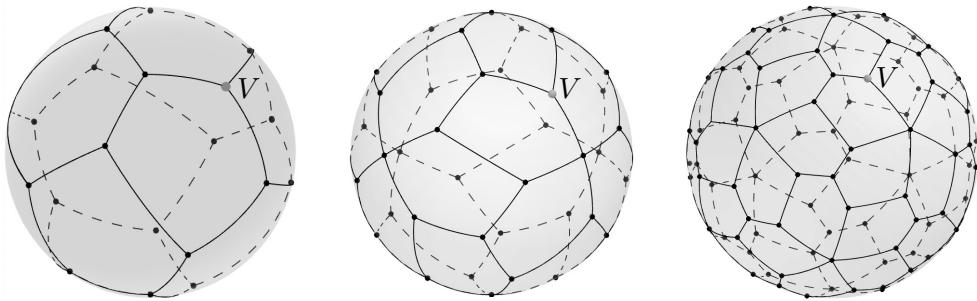


Figure 2: Pentagonal subdivision tilings with 12, 24, 60 tiles.

The construction of the pentagonal subdivision starts with an *anchor point* V indicated by \bullet . We connect V to A by the arc of length $< \pi$ (the other arc has length $> \pi$) to get a_1 , and then rotate a_1 around A by $-\frac{2}{3}\pi$ to get a_2 . On the other side, we connect V to B by the arc of length $< \pi$ to get b_1 , and then rotate b_1 around B by $\frac{2}{n}\pi$ to get b_2 . We further connect the other ends of a_2 and b_2 by arcs of length $< \pi$ to C . It turns out the two arcs form one arc c , and C is the middle point of c .

A tiling of the sphere by congruent polygons requires all the tiles to be simple, in the sense that the boundary of each tile is a simple closed curve [5, Lemma 1]. This is the reason for the $< \pi$ requirement in the construction above. Therefore the moduli space is the set of all V , such that the corresponding pentagon is simple.

Theorem. *The moduli space of pentagonal subdivision tilings is given by the locations of the anchor point in an open region of the sphere bounded by two arcs and three curves in Figure 19.*

Each of the three curves can be interpreted in two ways. The first is the intersection of a hyperbolic cylinder with the sphere. The second is the intersection of a quadratic cone (i.e., quadratic homogeneous equation) with the sphere. See the remark after (2.5). Their explicit formulae are obtained by simple transformations of the general form given by (2.6) through (2.9).

In Section 1, we divide the sphere into a number of regions, and discuss which regions are completely inside or outside the moduli space. The remaining regions only have some parts contained in the moduli space. In Section 2, we derive the formulae of the boundary of the moduli space parts in these remaining regions, in preferred stereographic projections (called A - and B -projections). In Section 3, we draw perspective pictures of the moduli space in the preferred stereographic M -projection, by using Möbius transforms to translate data in Section 2. In the final Section 4, we discuss various features of the moduli space, including the upper bounds of the edges, the reductions by the equalities of edge lengths, and the size of the moduli space. We explicitly express the areas of the three moduli spaces in terms of elliptic integrals. They are roughly 21.5%, 11.5%, 4.9% of the total area of the sphere.

All calculations are done by symbolic calculation software. All pictures are either real 3D pictures or of the perspective view (except the first of Figure 1, and Figure 17), with curves drawn in parameterized form. All non-decimal values are precise. The decimal values such as $R = 0.53308$ mean $0.53308 \leq R < 0.53309$. The only exception is the decimal values

in Table 3, where $\sup a = 0.6259072384\pi$ mean $0.6259072383\pi < \sup a < 0.6259072384\pi$. The obvious reason for the exception is that the values in the table must be upper bounds.

1 Moduli Space Region

We first determine the rough location of the anchor point V . The triangle $\triangle ABC$ in Figure 1 is one sixth of one regular triangular face of the Platonic solid. The angles at A, B, C are respectively $\frac{1}{3}\pi, \frac{1}{n}\pi, \frac{1}{2}\pi$. We rotate the great circle $\bigcirc AB$ around A by multiples of $\frac{1}{3}\pi$ to divide the sphere into six regions. We also rotate the great circle $\bigcirc AB$ around B by multiples of $\frac{1}{n}\pi$ to divide the sphere into $2n$ regions. The intersections of the two divisions divide the sphere into $6n$ regions.

We use stereographic projections (see Section 2.1) to describe what happens on the sphere. A stereographic projection is determined by its origin X and the direction of the real axis, which we call X -*projection*. We denote the antipode of P by P^* . In our pictures, all circles (and straight lines) are *arcs*, which are parts of great circles on the sphere. In a stereographic projection, we may visually determine arcs by the fact that arcs passing through P are exactly circles passing through both P and P^* .

We draw the division of the sphere in both A -projection and B -projection. The former is convenient for visualising the rotation from a_1 to a_2 , and the later is convenient for visualising the rotation from b_1 to b_2 . Figure 3 gives the perspective pictures of the two stereographic projections for the regular tetrahedron. We label the regions by $\Omega_1, \Omega_2, \dots, \Omega_{18}$. We also indicate A, B, C, M and their antipodes.

Figure 4 shows the A -projection of the pentagon when V lies in $\Omega_1, \Omega_2, \Omega_3, \Omega_7$. The first is the case $V \in \Omega_1$. We have $a_1, b_1 \in \Omega_1$. This implies $a_2, c_1 \in \Omega_4$ and $b_2, c_2 \in \Omega_8$. The locations of these arcs imply that the pentagon is simple. Similarly, for $V \in \Omega_2$, we have $a_1, b_1 \in \Omega_2$, $a_2, c_1 \in \Omega_4 \cup \Omega_6$, $b_2, c_2 \in \Omega_8 \cup \Omega_{14}$. For $V \in \Omega_3$, we have $a_1, b_1 \in \Omega_1 \cup \Omega_3$, $a_2, c_1 \in \Omega_2$, $b_2, c_2 \in \Omega_8 \cup \Omega_{10}$. For $V \in \Omega_7$, we have $a_1, b_1 \in \Omega_1 \cup \Omega_7$, $a_2, c_1 \in \Omega_4 \cup \Omega_{10}$, $b_2, c_2 \in \Omega_2$. All imply that the pentagon is simple. Two particular such pentagonal subdivision tilings are shown in the first two 3D pictures of Figure 5.

We also consider the extreme case that V lies on the boundaries of these regions. The pentagon is not simple exactly when V is any of the vertices of

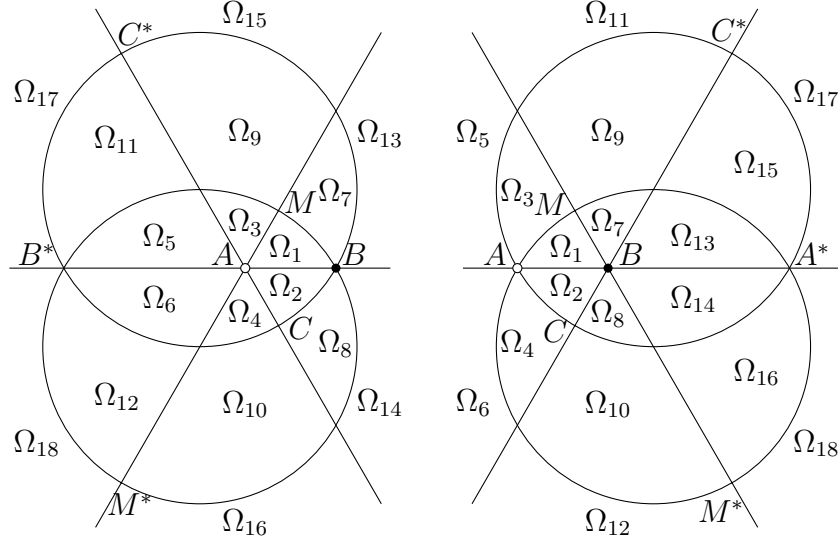


Figure 3: A- and B-projections of 18 regions for the tetrahedron.

$\Omega_1, \Omega_2, \Omega_3, \Omega_7$, or V is in the edges $\Omega_3 \cap \Omega_9$ (b_2, c_2 overlap) or $\Omega_7 \cap \Omega_9$ (a_2, c_1 overlap).

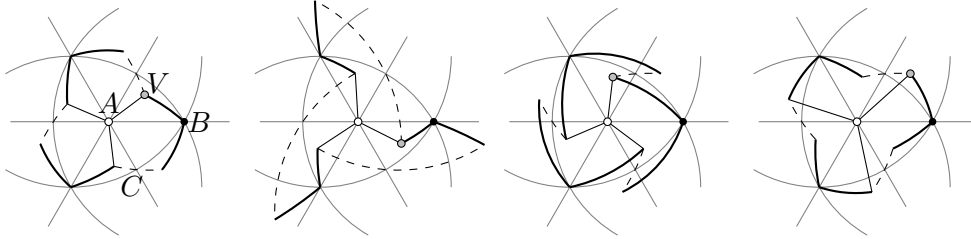


Figure 4: The pentagon is simple when V is in $\Omega_1, \Omega_2, \Omega_3, \Omega_7$.

Next we show that the pentagon is not simple when V is in some other regions. If $V \in \Omega_9$, then $a_1 \in A-3-9$, which means that a_1 starts from A and then successively passes through Ω_3, Ω_9 . Using the A-projection in Figure 3, we may deduce $a_2 \in A-2-8$ or $a_2 \in A-2-8-14$. We abbreviate this by writing $a_2 \in A-2-8-\dots$. Similarly, we have $b_1 \in B-7-9$. Using the B-projection, we get $b_2 \in B-2-4-\dots$. Since a curve in the direction $A-2-8$ and a curve in the direction $B-2-4$ must intersect (the intersection point is inside Ω_2), we conclude that a_2, b_2 intersect, and the pentagon is not simple.

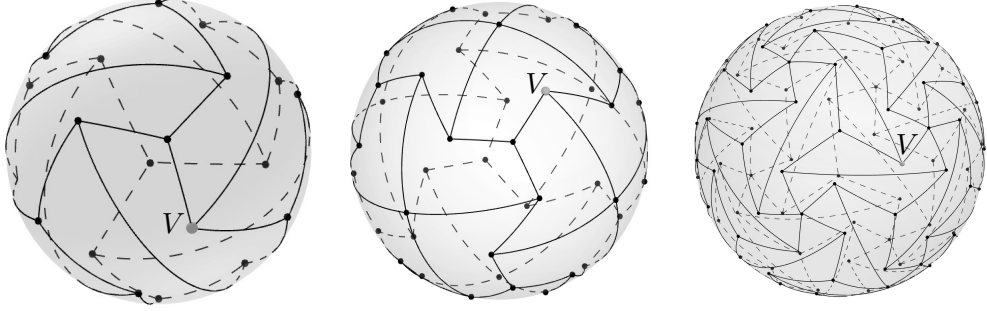


Figure 5: Pentagonal subdivision tilings when V is in Ω_2, Ω_3 , or part of Ω_8 .

Similar argument shows that the pentagon is not simple in the following cases. We indicate the two intersecting edges.

- $V \in \Omega_9$: $a_2 \in A - 2 - 8 - \dots$, $b_2 \in B - 2 - 4 - \dots$.
- $V \in \Omega_{11}$: $a_2 \in A - 1 - 7 - 13$, $b_1 \in B - 7 - 9 - 11$.
- $V \in \Omega_{15}$: $a_1 \in A - 3 - 9 - 15$, $b_2 \in B - 1 - 3 - 5$.
- $V \in \Omega_{17}$: $a_2 \in A - 1 - 7 - 13$, $b_2 \in B - 1 - 3 - 5$.
- $V \in \Omega_6$: $b_1 \in B - 2 - 4 - 6$, $c_1 \in C - 2 - 1 - \dots$.
- $V \in \Omega_{10}$: $a_1 \in A - 4 - 10$, $c_1 \in C - 4 - 6 - 5 - 11$.
- $V \in \Omega_{12}$: $b_1 \in B - 8 - 10 - 12$, $c_2 \in C - 10 - 16 - 17$.
- $V \in \Omega_{14}$: $a_1 \in A - 2 - 8 - 14$, $c_2 \in C - 2 - 1 - (3/7) - 9$. Here $(3/7)$ means the arc passes through Ω_3 or Ω_7 .
- $V \in \Omega_{16}$: $a_1 \in A - 4 - 10 - 16$, $c_1 \in C - 10 - 12 - 18 - 17$.
- $V \in \Omega_{18}$: $a_2 \in A - 3 - 9 - 15$, $b_2 \in B - 7 - 9 - 11$.

For the pentagonal subdivision of the tetrahedron, it remains to study the regions $\Omega_4, \Omega_5, \Omega_8, \Omega_{13}$. Figure 6 shows that it is possible for the pentagon to be simple if V is in certain parts of these regions. The third of Figure 5 shows the 3D picture of one such pentagonal subdivision tiling. We calculate these regions in Section 2.

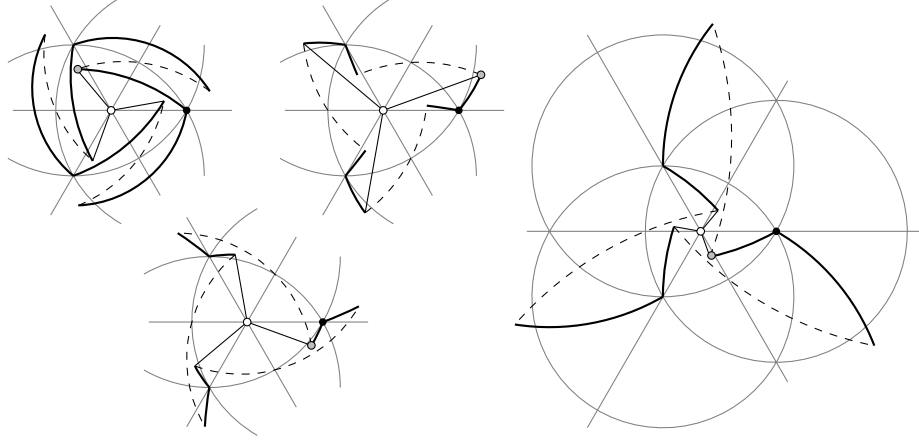


Figure 6: The pentagon is simple when V is in certain parts of $\Omega_5, \Omega_{13}, \Omega_8, \Omega_4$.

We may carry out similar region by region argument for the pentagonal subdivision of the octahedron. Figure 7 is the two stereographic projections for the regular octahedron. We simplify the presentation by labelling the regions by i instead of Ω_i . If V is in $\Omega_1, \Omega_2, \Omega_3, \Omega_7$, then the same argument shows that the pentagon is simple. Moreover, the pentagon is not simple if V is a vertex of these regions, or is in $\Omega_3 \cap \Omega_9$ or $\Omega_7 \cap \Omega_9$.

If V is in the following regions, then the pentagon is not simple. Again, we indicate the two intersecting edges.

- $V \in \Omega_9$: $a_2 \in A - 2 - 8 - \dots$, $b_2 \in B - 2 - 4 - \dots$.
- $V \in \Omega_{11}$: $a_2 \in A - 1 - 7 - 13 - 19$, $b_1 \in B - 7 - 9 - 11$.
- $V \in \Omega_{15}$: $a_1 \in A - 3 - 9 - 15$, $b_2 \in B - 1 - 3 - 5$.
- $V \in \Omega_{17}$: $a_2 \in A - 1 - 7 - 13 - 19$, $b_1 \in B - 13 - 15 - 17$.
- $V \in \Omega_{21}$: $a_1 \in A - 3 - 9 - 15 - 21$, $b_2 \in B - 7 - 9 - 11$.
- $V \in \Omega_{23}$: $a_2 \in A - 1 - 7 - 13 - 19$, $b_2 \in B - 7 - 9 - 11$.
- $V \in \Omega_6$: $b_1 \in B - 2 - 4 - 6$, $c_1 \in C - 2 - 1 - \dots$.
- $V \in \Omega_{10} \cup \Omega_{16}$: $a_1 \in A - 4 - 10 - \dots$, $c_1 \in C - 4 - 6 - \dots$.
- $V \in \Omega_{20}$: $a_1 \in A - 2 - 8 - 14 - 20$, $c_2 \in B - 2 - 1 - \dots$.

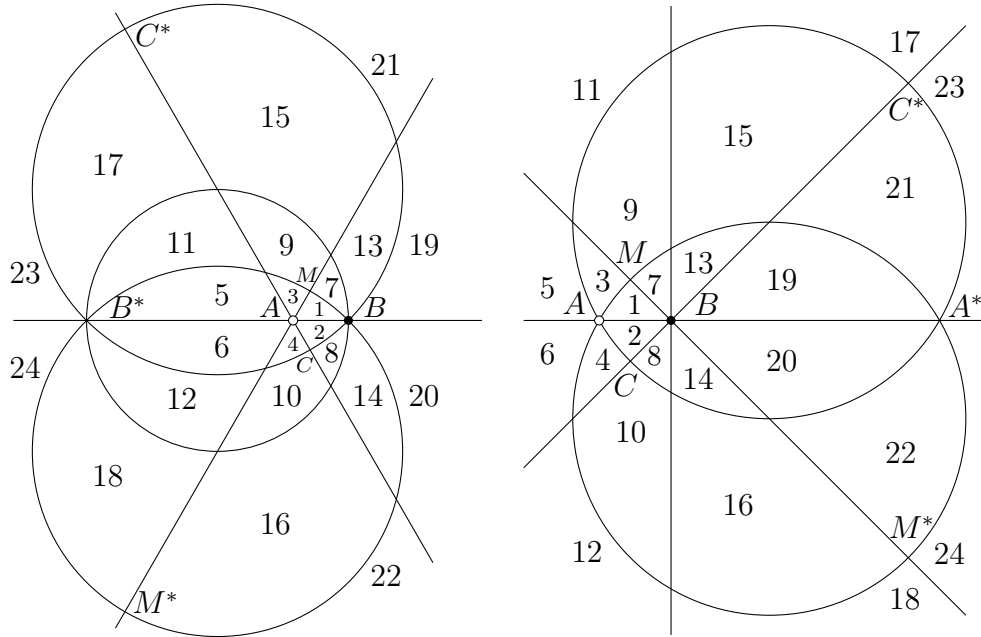


Figure 7: A- and B-projections of 24 regions for the octahedron.

- $V \in \Omega_{22}$: $a_1 \in A - 4 - 10 - 16 - 22$, $b_2 \in B - 8 - 10 - 12$.
- $V \in \Omega_{24}$: $a_2 \in A - 3 - 9 - 15 - 21$, $b_2 \in B - 13 - 15 - 17$.

For some other regions, we need to use the following geometric lemma to show that the pentagon is not simple.

Lemma 1. *Suppose P and P^* are a pair of antipodal points, and $P^*X > PX$ and $VX = WX$ in Figure 8.*

1. *If $\rho \leq \frac{1}{2}\pi$ and $\theta^* \leq \theta$, then WX and PV intersect.*
2. *If $\rho \geq \frac{1}{2}\pi$ and $\theta^* \geq \theta$, then WX and PV intersect.*

Figure 8 is the X -projection. The lines are arcs, the dashed line is a half circle, and all angles are positive. It is easy to see the validity of the lemma in the Euclidean metric of $\mathbb{C} = \mathbb{R}^2$ (PXP^* , VX , WX are literally straight lines). We note that, in the X -projection, $P^*X > PX$ and $VX = WX$ in the Euclidean metric are equivalent to the same (in)equalities in the spherical metric. Since the stereographic projection preserves the angles, the lemma is

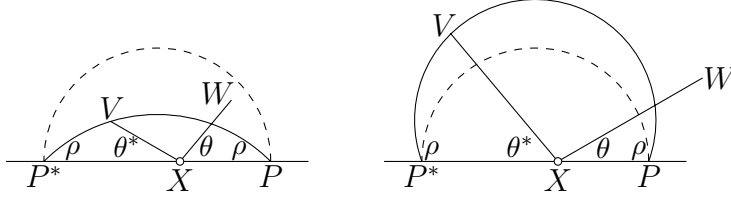


Figure 8: A geometric lemma, presented in X -projection.

actually valid on the sphere, and therefore is also valid in any stereographic projection as long as the lengths are understood to be spherical.

Applying Lemma 1, the pentagon is not simple in the following cases.

- $V \in \Omega_{12}$: $X = B$, $P = C$, $\rho \geq \frac{1}{2}\pi$, $\theta^* \geq \frac{1}{4}\pi \geq \theta$, $WX = b_1$, $PV = c_2$.
- $V \in \Omega_{14}$: $X = B$, $P = C$, $\rho \leq \frac{1}{2}\pi$, $\theta^* \leq \frac{1}{4}\pi \leq \theta$, $WX = b_1$, $PV = c_2$.
- $V \in \Omega_{18}$: $X = B$, $P = C$, $\rho \geq \frac{1}{2}\pi$, $\theta^* \geq \frac{1}{4}\pi \geq \theta$, $WX = b_1$, $PV = c_2$.
- $V \in \Omega_{19}$: $X = B$, $P = C$, $\rho \leq \frac{1}{2}\pi$, $\theta^* \leq \frac{1}{4}\pi \leq \theta$, $WX = b_2$, $PV = a_1$.

Again it remains to study the regions $\Omega_4, \Omega_5, \Omega_8, \Omega_{13}$ for the pentagonal subdivision of the octahedron.

Figures 9 and 10 are the two stereographic projections for the icosahedron. If V is in $\Omega_1, \Omega_2, \Omega_3, \Omega_7$, then the same argument shows that the pentagon is simple. Moreover, the pentagon is not simple if V is a vertex of these regions, or is in $\Omega_3 \cap \Omega_9$ or $\Omega_7 \cap \Omega_9$.

If V is in the following regions, then the pentagon is not simple.

- $V \in \Omega_9$: $a_2 \in A - 2 - 8 - \dots$, $b_2 \in B - 2 - 4 - \dots$.
- $V \in \Omega_{11}$: $a_2 \in A - 1 - 7 - 13 - 19 - 25$, $b_1 \in B - 7 - 9 - 11$.
- $V \in \Omega_{15}$: $a_1 \in A - 3 - 9 - 15$, $b_2 \in B - 1 - 3 - 5$.
- $V \in \Omega_{17}$: $a_2 \in A - 1 - 7 - 13 - 19 - 25$, $b_1 \in B - 13 - 15 - 17$.
- $V \in \Omega_{21}$: $a_1 \in A - 3 - 9 - 15 - 21$, $b_2 \in B - 7 - 9 - 11$.
- $V \in \Omega_{23}$: $a_2 \in A - 1 - 7 - 13 - 19 - 25$, $b_2 \in B - 7 - 9 - 11$.
- $V \in \Omega_{27}$: $a_1 \in A - 3 - 9 - 15 - 21 - 27$, $b_2 \in B - 13 - 15 - 17$.

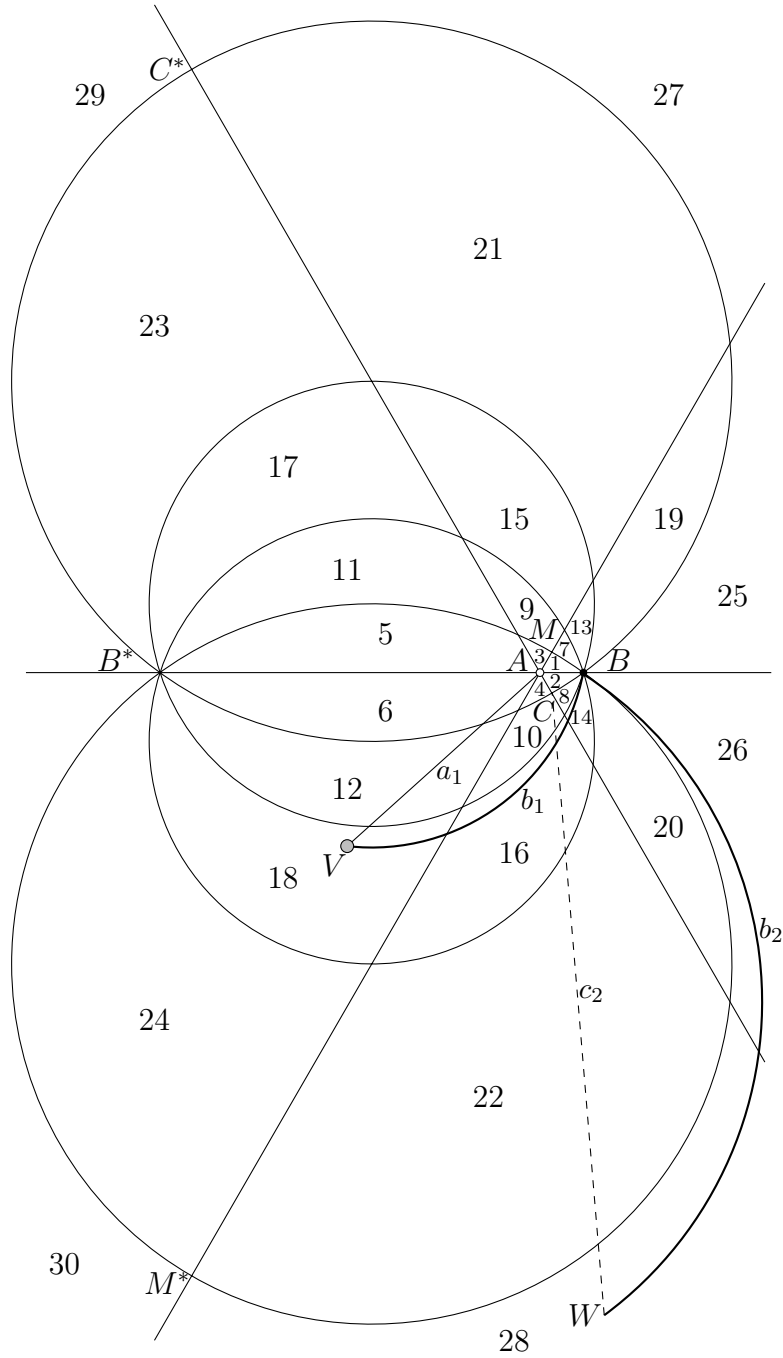


Figure 9: A -projections of 30 regions for the icosahedron, and the case $V \in \Omega_{18}$.

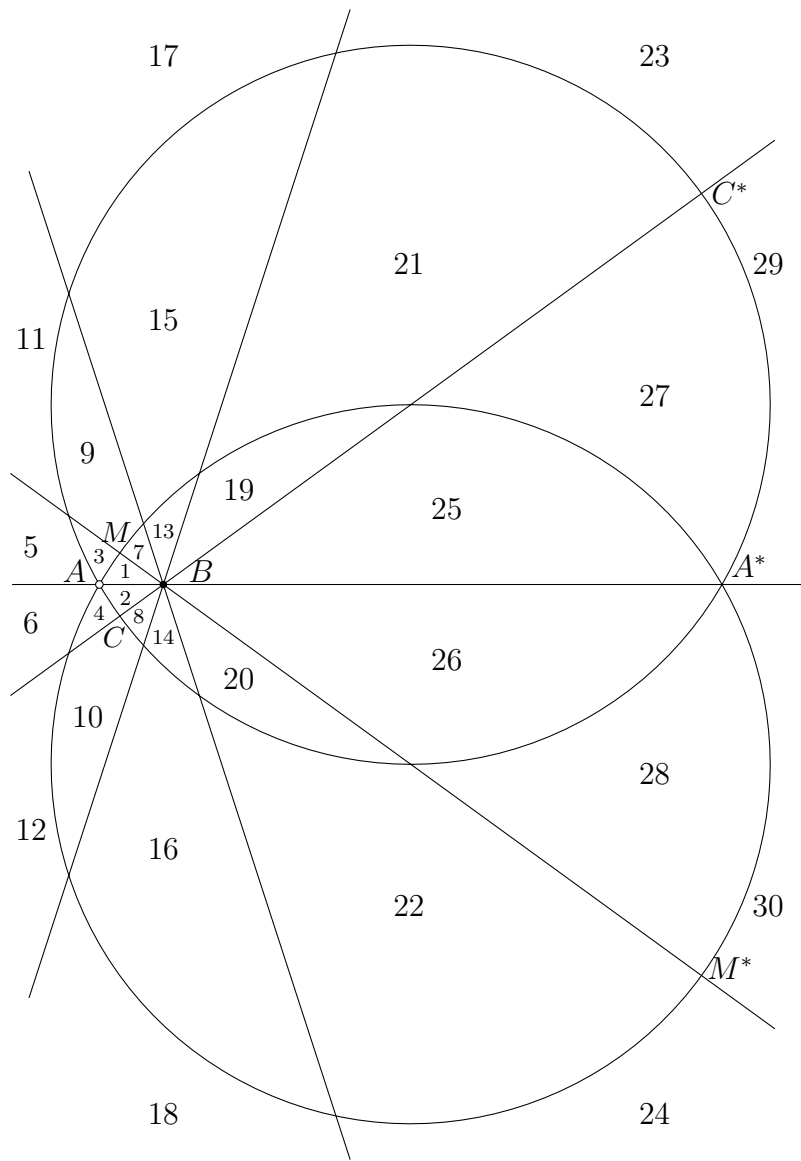


Figure 10: B -projections of 30 regions for the icosahedron.

- $V \in \Omega_{29}$: $a_2 \in A - 1 - 7 - 13 - 19 - 25$, $b_2 \in B - 13 - 15 - 17$.
- $V \in \Omega_6$: $b_1 \in B - 2 - 4 - 6$, $c_1 \in C - 2 - 1 - \dots$.
- $V \in \Omega_{10} \cup \Omega_{16} \cup \Omega_{22}$: $a_1 \in A - 4 - 10 - \dots$, $c_1 \in C - 4 - 6 - \dots$.
- $V \in \Omega_{26}$: $a_1 \in A - 2 - 8 - 14 - 20 - 26$, $c_2 \in C - 2 - 1 - \dots$.
- $V \in \Omega_{30}$: $a_2 \in A - 3 - 9 - 15 - 21 - 27$, $b_2 \in B - 19 - 21 - 23$.

Applying Lemma 1, the pentagon is not simple in the following cases.

- $V \in \Omega_{12}$: $X = B$, $P = C$, $\rho \geq \frac{1}{2}\pi$, $\theta^* \geq \frac{2}{5}\pi \geq \theta$, $WX = b_1$, $PV = c_2$.
- $V \in \Omega_{20}$: $X = B$, $P = C$, $\rho \leq \frac{1}{2}\pi$, $\theta^* \leq \frac{2}{5}\pi \leq \theta$, $WX = b_1$, $PV = c_2$.
- $V \in \Omega_{25}$: $X = B$, $P = A$, $\rho \leq \frac{1}{2}\pi$, $\theta^* \leq \frac{2}{5}\pi \leq \theta$, $WX = b_2$, $PV = a_1$.

For $V \in \Omega_{18}, \Omega_{24}, \Omega_{29}$, we observe the following.

- $V \in \Omega_{18}$: $a_1 \in A - 6 - 12 - 18$, $b_1 \in B - 14 - 16 - 18$. The two ends of b_2 are B and W , with $W \in \Omega_{26} \cup \Omega_{28} \cup \Omega_{30}$. See Figure 9.
- $V \in \Omega_{24}$: $a_1 \in A - 6 - 12 - 18 - 24$, $b_1 \in B - 20 - 22 - 24$. The two ends of b_2 are B and W , with $W \in \Omega_{29}$.
- $V \in \Omega_{28}$: $a_1 \in A - 4 - 10 - 16 - 22 - 28$, $b_1 \in B - 26 - 28$. The two ends of a_2 are A and W , with $W \in \Omega_{29}$.

We note that C is inside the triangle \triangle_C bounded by a_1, b_1 and AB , and W is outside the triangle. Therefore CW intersects the boundary of \triangle_C . Since CW is c_2 for $V \in \Omega_{18}, \Omega_{24}$, and CW is c_1 for $V \in \Omega_{28}$, we know c does not intersect a_1 and b_1 . Therefore CW intersect AB .

On the other hand, for the case $V \in \Omega_{18}$, C and W are in the same side of AB (i.e., both points are in the same semisphere divided by the great circle $\circ AB$). For the case $V \in \Omega_{24}, \Omega_{28}$, B and W are in different sides of AC (i.e., the two points are in different semispheres divided by the great circle $\circ AC$). Both properties imply that CW does not intersect AB .

It remains to study the regions $\Omega_4, \Omega_5, \Omega_8, \Omega_{13}, \Omega_{14}, \Omega_{19}$ for the pentagonal subdivision of the icosahedron.

2 Boundary of Moduli Space

For tetrahedron and octahedron, it remains to consider V in $\Omega_4, \Omega_5, \Omega_8, \Omega_{13}$. For icosahedron, it remains to consider V in $\Omega_4, \Omega_5, \Omega_8, \Omega_{13}, \Omega_{14}, \Omega_{19}$. The anchor point V must be in certain parts of these regions for the pentagon to be simple. The parts are calculated in suitable stereographic projections.

2.1 Stereographic Projection

We parameterise a stereographic projection by complex numbers, such that the equator is the circle $z\bar{z} = 1$ of radius 1 centered at 0. See Figure 11. Under the projection, a point $\xi = (\xi_{12}, \xi_3) = (\xi_1, \xi_2, \xi_3)$ on the sphere and its complex paramaterisation $z = re^{i\theta}$ are related by

$$\xi = \frac{(2re^{i\theta}, r^2 - 1)}{r^2 + 1} = \frac{(2z, |z|^2 - 1)}{|z|^2 + 1}, \quad z = \frac{\xi_{12}}{1 - \xi_3}, \quad |z|^2 = \frac{1 + \xi_3}{1 - \xi_3}.$$

For the convenience of writing the formulae for the boundaries of the moduli spaces in the later discussion, we introduce R by (see (2.7) and (2.8))

$$r^{-1} - r = 2R, \quad r = \sqrt{R^2 + 1} - R. \quad (2.1)$$

Then we have

$$\xi = \frac{(e^{i\theta}, -R)}{\sqrt{R^2 + 1}} = \frac{(\cos \theta, \sin \theta, -R)}{\sqrt{R^2 + 1}}. \quad (2.2)$$

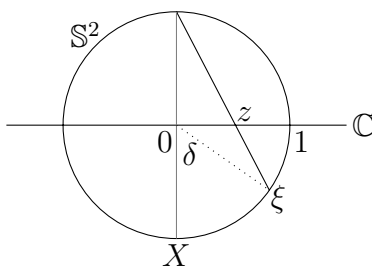


Figure 11: X -projection.

The antipode z^* of z is given by $z^*\bar{z} = -1$. The spherical distance δ between X and ξ satisfies $\tan \frac{1}{2}\delta = |z|$. The parameterisations of different projections are related by Möbius transforms.

We use z_X to denote the parameterisation by the X -projection. For example, we write a Möbius transform from X -projection to Y -projection as

$$z_Y = \frac{az_X + b}{cz_X + d}.$$

Moreover, we denote by $Y_X \in \mathbb{C}$ the X -projection of $Y \in \mathbb{S}^2$. Then we always have $X_X = 0$ and $X_X^* = \infty$. The geometry shows that the Euclidean distance $|Y_X|$ (norm of complex number) of X and Y in the X -projection is equal to the Euclidean distance $|X_Y|$ of X and Y in the Y -projection. We denote $d_{XY} = |Y_X| = |X_Y|$.

Our description of the moduli space is based on the triangle $\triangle ABM$, which is the region Ω_1 in Section 1. The triangle has angles $\frac{1}{3}\pi, \frac{1}{n}\pi, \frac{1}{2}\pi$ at A, B, M . We will use the following projections:

- A -projection: B is in the positive real direction.
- B -projection: A is in the negative real direction.
- M -projection: A is in the negative real direction.

Moreover, the direction $A \rightarrow B \rightarrow M$ is always counterclockwise. This implies that M is in the upper half of the A - and B -projections, and B is in the lower half (in fact the negative imaginary direction) of the M -projection.

The first of Figure 12 is the triangle $\triangle ABM$ in the A -projection. We have

$$B_A = d_{AB}, \quad B_A^* = -\bar{B}_A^{-1} = -d_{AB}^{-1}, \quad M_A = d_{AM}e^{i\frac{1}{3}\pi},$$

and BMB^* is a circle centered at O . Then the middle point D of B and B^* has $D_A = \frac{1}{2}(d_{AB} - d_{AB}^{-1})$. This gives the Euclidean distances in the A -projection (indicated by subscript A)

$$|AD|_A = \frac{1}{2}(d_{AB}^{-1} - d_{AB}), \quad |BD|_A = \frac{1}{2}(d_{AB}^{-1} + d_{AB}).$$

By $\angle OAD = \frac{1}{3}\pi$ and $\angle OBD = \frac{1}{2}\pi - \angle ABM = (\frac{1}{2} - \frac{1}{n})\pi$, we may calculate the distance $|OD|_A$ in two ways and get an equation

$$(d_{AB}^{-1} - d_{AB}) \tan \frac{1}{3}\pi = (d_{AB}^{-1} + d_{AB}) \tan(\frac{1}{2} - \frac{1}{n})\pi.$$

We solve the equation and get one positive solution

$$d_{AB} = \sqrt{\frac{\sqrt{3} \tan \frac{1}{n}\pi - 1}{\sqrt{3} \tan \frac{1}{n}\pi + 1}}.$$

The explicit values are given in Table 1. Then we further get

$$\begin{aligned}
d_{AM} &= |OM|_A - |OA|_A = |OB|_A - |OA|_A \\
&= |BD|_A \sec\left(\frac{1}{2} - \frac{1}{n}\right)\pi - |AD|_A \sec \frac{1}{3}\pi \\
&= \frac{1}{2}(d_{AB}^{-1} + d_{AB}) \sec\left(\frac{1}{2} - \frac{1}{n}\right)\pi - \frac{1}{2}(d_{AB}^{-1} - d_{AB}) \sec \frac{1}{3}\pi.
\end{aligned}$$

	$n = 3$ tetrahedron	$n = 4$ octahedron	$n = 5$ icosahedron
d_{AB}	$\frac{1}{\sqrt{2}}$	$\frac{\sqrt{3}-1}{\sqrt{2}}$	$\frac{1}{4}(\sqrt{30} + 6\sqrt{5} - \sqrt{5} - 3)$
d_{AM}	$\frac{\sqrt{3}-1}{\sqrt{2}}$	$\sqrt{3} - \sqrt{2}$	$\frac{1}{2}(\sqrt{15} - \sqrt{5} + \sqrt{3} - 3)$
d_{BM}	$\frac{\sqrt{3}-1}{\sqrt{2}}$	$\sqrt{2} - 1$	$\frac{1}{2}(\sqrt{10} + 2\sqrt{5} - \sqrt{5} - 1)$

Table 1: Euclidean distances.

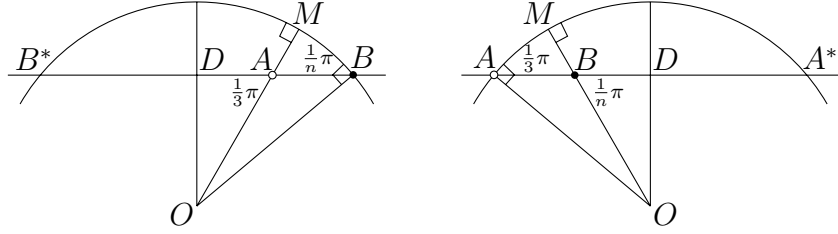


Figure 12: Calculate $\triangle ABM$ in the A - and B -projections.

To get d_{BM} , we use the second of Figure 12, which is the triangle $\triangle ABM$ in the B -projection. By

$$A_B = -d_{AB}, \quad A_B^* = d_{AB}^{-1}, \quad M_B = d_{BM} e^{i(1-\frac{1}{n})\pi},$$

we similarly get

$$\begin{aligned}
d_{BM} &= |OM|_B - |OB|_B = |OA|_B - |OB|_B \\
&= |BD|_B \sec\left(\frac{1}{2} - \frac{1}{3}\right)\pi - |AD|_B \sec \frac{1}{n}\pi \\
&= \frac{1}{2}(d_{AB}^{-1} + d_{AB}) \sec \frac{1}{6}\pi - \frac{1}{2}(d_{AB}^{-1} - d_{AB}) \sec \frac{1}{n}\pi.
\end{aligned}$$

Again the explicit values are given in Table 1.

2.2 Determination of Boundary

In Figure 13, for $v \in \Omega_5$, we connect Av and rotate by $-\frac{2}{3}\pi$ around A to get Aw . The picture is for the tetrahedron in A -projection, and is schematically correct for the octahedron and icosahedron. In this construction, we have $Av = a_1$, $Aw = a_2$ and $Bv = b_1$.

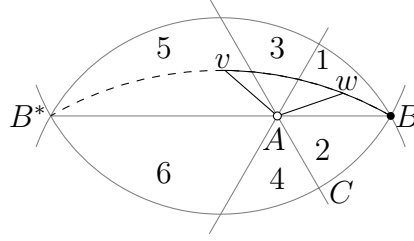


Figure 13: Boundary of the moduli space part in Ω_5 .

If Aw intersects Bv , then the pentagon is not simple, and v is not in the moduli space. If Aw does not intersect Bv , then by $b_2 \in B - 8 - 10$, $c_1 \in C - 2 - 1$, and $c_2 \in C - 10$, we know the pentagon is simple. The critical case between the two cases is when B, w, v, B^* are on the same great circle. This means that the end w of a_2 touches b_1 .

Figure 14 gives the general description. In the X -projection, let P be the point at d satisfying $0 < d < 1$. Then the antipode $P^* = -d^{-1}$. We also fix a rotation angle 2α , with $\alpha \in (0, \frac{1}{2}\pi)$. Then we look for $v = re^{i\phi}$, $w = ve^{-i2\alpha} = re^{i(\phi-2\alpha)}$, $r > 0$, such that P, w, v, P^* are on the same great circle. We assume that both v and w are in the upper half, which means $\phi \in [2\alpha, \pi]$. We also assume that the arc $PwvP^*$ is the “shorter” (actually the same length on the sphere) of the two arcs connecting P and P^* . This corresponds to $\rho < \frac{1}{2}\pi$ in Lemma 1. By the lemma, we must have $\phi \in [2\alpha, \frac{1}{2}\pi + \alpha]$.

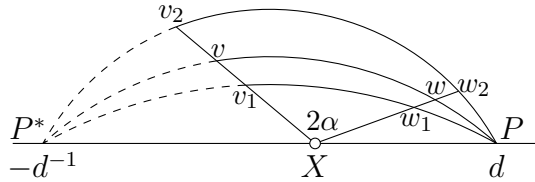


Figure 14: Determine the boundary curve of the moduli space.

Lemma 2. *In Figure 14, suppose $XP < XP^*$, and P, w, v, P^* are on the same great circle. Suppose v_1, v_2 are two points on the ray Xv , such that v_1 is within v and v_2 is beyond v , and $\angle XPv_2 < \frac{1}{2}\pi$. Suppose w_1, w_2 are the intersections of Pv_1, Pv_2 with the ray Xw . Then $Xv_1 < Xw_1$ and $Xv_2 > Xw_2$.*

In the lemma, the inequalities in the Euclidean metric are equivalent to the same inequalities in the spherical metric. Therefore the lemma holds on the sphere.

The proof of the lemma is given by Figure 15. The first picture expands the spheres $\odot Pv_1P^*$, $\odot PvP^*$, $\odot Pv_2P^*$ in Figure 14. Their respective centers O_1, O, O_2 are arranged on the same straight line as in the picture. Then we get the situation in the second picture, in which the circle is $\odot Pv_1P^*$ or $\odot Pv_2P^*$, and we may assume OX is a horizontal line above the center of the circle. From X , we shoot two rays at angles $\pm\alpha$ with respect to OX , and the two rays intersect the circle at V, W . Then Lemma 2 effectively means $XV > XW$. To see the inequality, we flip the circle with respect to OX and get a new circle. Since OX is above the center of the circle, the new circle intersects XV at W' . Then we get $XW = XW' < XV$. This completes the proof of Lemma 2.

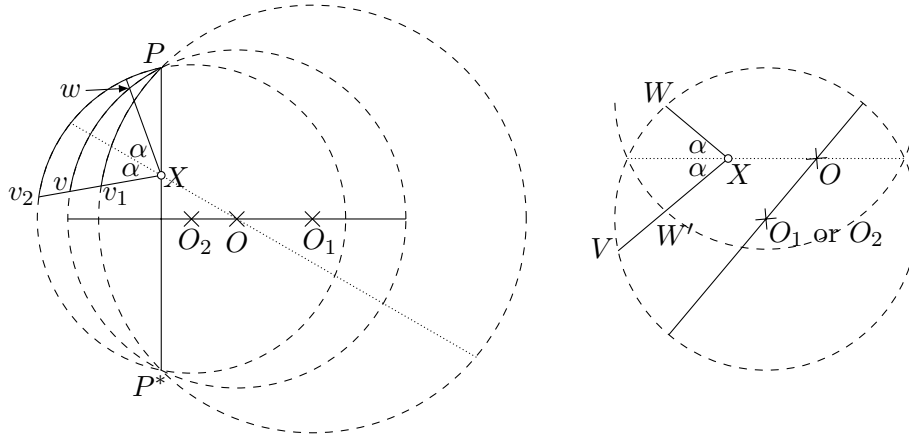


Figure 15: Proof of Lemma 2.

We apply Lemma 2 to Figure 13. For any $\phi \in [2\alpha, \frac{1}{2}\pi + \alpha]$, $\alpha = \frac{1}{3}\pi$, we consider the ray from A at angle $\phi = \angle BA v$. There is a point v on the ray, such that B, w, v, B^* are on the same circle. Then Lemma 2 says that a point on the ray is inside the moduli space if and only if it is between A

and v . Therefore the track of v in Figure 13 gives a curve γ_A . The part of the moduli space in Ω_5 is the region between A and γ_A (not including the curve), and is bounded by γ_A and the arc $\Omega_3 \cap \Omega_5$ (including the interior of the arc).

2.3 Formula for Boundary

In Figure 14, the four points $v = re^{i\phi}$, $w = ve^{-i2\alpha} = re^{i(\phi-2\alpha)}$, $P = d$, $P^* = -d^{-1}$ are on the same great circle if and only if the following is a real number ($=_{\mathbb{R}}$ means equality up to multiplying and adding real numbers)

$$\begin{aligned} \frac{v + d^{-1}}{v - w} \cdot \frac{d - w}{d + d^{-1}} &=_{\mathbb{R}} \frac{(v + d^{-1})(d - ve^{-i2\alpha})}{v(1 - e^{-i2\alpha})} \\ &=_{\mathbb{R}} i((d - d^{-1}) \cos \alpha - ve^{-i\alpha} + v^{-1}e^{i\alpha}). \end{aligned}$$

The condition for the number to be real is a cubic equation

$$4\lambda|v|^2 + (ve^{-i\alpha} + \bar{v}e^{i\alpha})(|v|^2 - 1) = 0, \quad (2.3)$$

where

$$\lambda = \frac{1}{2}(d^{-1} - d) \cos \alpha > 0. \quad (2.4)$$

In terms of $\xi = (\xi_1, \xi_2, \xi_3)$ on the sphere, the equation (2.3) for the track γ of v becomes quadratic

$$\lambda(1 - \xi_3^2) + (\xi_1 \cos \alpha + \xi_2 \sin \alpha)\xi_3 = \lambda(\xi_1^2 + \xi_2^2) + (\xi_1 \cos \alpha + \xi_2 \sin \alpha)\xi_3 = 0. \quad (2.5)$$

The first version is a hyperbolic cylinder, and the second version is homogeneous. Therefore the curve is the intersection of a hyperbolic cylinder with the sphere, and is also the intersection of a quadratic cone with the sphere.

For $v = x + iy$, (2.3) becomes the cartesian form of γ

$$2\lambda(x^2 + y^2) + (x \cos \alpha + y \sin \alpha)(x^2 + y^2 - 1) = 0. \quad (2.6)$$

For $v = re^{i\phi}$, γ is a curve connecting $de^{i2\alpha}$ to 0, given by (see (2.1))

$$r^{-1} - r = 2R = 2\lambda \sec(\phi - \alpha), \quad \phi \in [2\alpha, \frac{1}{2}\pi + \alpha]. \quad (2.7)$$

The formula implies that $R > 0$ and is strictly increasing in ϕ . This implies that $1 > r > 0$, and r is strictly decreasing in ϕ . Then we take the non-negative solution of (2.7) to get the explicit formula

$$r = \sqrt{\lambda^2 \sec^2(\phi - \alpha) + 1} - \lambda \sec(\phi - \alpha), \quad \phi \in [2\alpha, \frac{1}{2}\pi + \alpha]. \quad (2.8)$$

By (2.2), we also get the spherical version of the curve

$$\xi = \frac{(\cos \phi, \sin \phi, -\lambda \sec(\phi - \alpha))}{\sqrt{\lambda^2 \sec^2(\phi - \alpha) + 1}}, \quad \phi \in [2\alpha, \frac{1}{2}\pi + \alpha]. \quad (2.9)$$

This is equivalent to (2.5).

We apply the calculation to γ_A . This means $X = A$, $P = B$, $\alpha = \frac{1}{3}\pi$, $d = d_{AB}$. Moreover, $z_A = re^{i\theta}$ equals $v = re^{i\phi}$. Substituting the data into (2.6) through (2.9), we get λ_A in Table 2 and the complex equation for the A -projection of γ_A

$$4\lambda_A |z|^2 + (ze^{-i\frac{1}{3}\pi} + \bar{z}e^{i\frac{1}{3}\pi})(|z|^2 - 1) = 0.$$

The cartesian equation for $z = x + iy$ is

$$4\lambda_A(x^2 + y^2) + (x + \sqrt{3}y)(x^2 + y^2 - 1) = 0.$$

The polar equation for $z = re^{i\theta}$ is

$$r = \sqrt{\lambda_A^2 \sec^2(\theta - \frac{1}{3}\pi) + 1} - \lambda_A \sec(\theta - \frac{1}{3}\pi), \quad \theta \in [\frac{2}{3}\pi, \frac{5}{6}\pi].$$

The spherical equation is

$$\xi = \frac{(\cos \theta, \sin \theta, -\lambda_A \sec(\theta - \frac{1}{3}\pi))}{\sqrt{\lambda_A^2 \sec^2(\theta - \frac{1}{3}\pi) + 1}}, \quad \theta \in [\frac{2}{3}\pi, \frac{5}{6}\pi].$$

	$n = 3$	$n = 4$	$n = 5$
$\lambda_A = \frac{1}{2}(d_{AB}^{-1} - d_{AB}) \cos \frac{1}{3}\pi$	$\frac{1}{4\sqrt{2}}$	$\frac{1}{2\sqrt{2}}$	$\frac{\sqrt{5+3}}{8}$
$\lambda_B = \frac{1}{2}(d_{AB}^{-1} - d_{AB}) \cos \frac{1}{n}\pi$	$\frac{1}{4\sqrt{2}}$	$\frac{1}{2}$	$\frac{\sqrt{5+2}}{4}$
$\lambda_C = \frac{1}{2}(d_{AM}^{-1} - d_{AM}) \cos \frac{1}{3}\pi$	$\frac{1}{2\sqrt{2}}$	$\frac{1}{\sqrt{2}}$	$\frac{\sqrt{5+3}}{4}$

Table 2: Coefficients for γ_A , γ_B , γ_C .

Next we apply the calculation to Ω_{13} (for $n = 3, 4$) or $\Omega_{13} \cup \Omega_{19}$ (for $n = 5$). The situation is similar to Ω_5 , with a and b exchanged. This means that A and B are exchanged, and the calculation can be done in the B -projection. We denote the track by γ_B , and $V \in \Omega_{13}$ (or $\Omega_{13} \cup \Omega_{19}$) gives a

simple pentagon if and only if V lies between γ_B (not including the curve) and the arc $\Omega_7 \cap \Omega_{13}$.

By comparing the B -projection with the A -projection, we may calculate γ_B by horizontally flipping the standard picture in Figure 14. This means taking $X = B$, $P = A$, $\alpha = \frac{1}{n}\pi$, $d = d_{AB}$. Moreover, for $z_B = re^{i\theta}$, we take $v = re^{i(\pi-\theta)} = -\bar{z}_B$. Substituting the data into (2.6) through (2.9), we get λ_B in Table 2 and the complex equation for the B -projection of γ_B

$$4\lambda_B|z|^2 - (ze^{i\frac{1}{n}\pi} + \bar{z}e^{-i\frac{1}{n}\pi})(|z|^2 - 1) = 0.$$

The cartesian equation is

$$2\lambda_B(x^2 + y^2) - (x \cos \frac{1}{n}\pi - y \sin \frac{1}{n}\pi)(x^2 + y^2 - 1) = 0.$$

The polar equation is

$$r = \sqrt{\lambda_B^2 \sec^2(\theta + \frac{1}{n}\pi) + 1} + \lambda_B \sec(\theta + \frac{1}{n}\pi), \quad \theta \in [(\frac{1}{2} - \frac{1}{n})\pi, (1 - \frac{2}{n})\pi].$$

The spherical equation is

$$\xi = \frac{(\cos \theta, \sin \theta, \lambda_B \sec(\theta + \frac{1}{n}\pi))}{\sqrt{\lambda_B^2 \sec^2(\theta + \frac{1}{n}\pi) + 1}}, \quad \theta \in [(\frac{1}{2} - \frac{1}{n})\pi, (1 - \frac{2}{n})\pi].$$

Next we apply the calculation to Ω_4 . This is described by Figure 16, which is the rotation of the first of Figure 3 by $-\frac{2}{3}\pi$. For $v \in \Omega_4$, we rotate v by $-\frac{2}{3}\pi$ around A to get w , and require C, v, w, C^* to be on the same great circle. If $V = v$, then $Av = a_1$, $Aw = a_2$, $Cw = c_1$, and the picture describes the extreme case that the end v of a_1 touches c_1 . The track of v gives a curve γ_C . By Lemma 2, a point $V \in \Omega_4$ gives a simple pentagon if and only if V lies between the curve γ_C (not including the curve) and the arc AC .

Matching Figure 16 with Figure 14 means taking $X = A$, $P = C$, $\alpha = \frac{1}{3}\pi$, $d = d_{AC} = d_{AM}$. Moreover, for $z_A = re^{i\theta}$, we take $v = re^{i(\frac{1}{3}\pi-\theta)} = \bar{z}_A e^{i\frac{1}{3}\pi}$ (note that v and w are exchanged in the matching of the two pictures). Substituting the data into (2.6) through (2.9), we get λ_C in Table 2 and the complex equation for the A -projection of γ_C

$$4\lambda_C|z|^2 + (z + \bar{z})(|z|^2 - 1) = 0.$$

The cartesian equation is

$$2\lambda_C(x^2 + y^2) + x(x^2 + y^2 - 1) = 0.$$

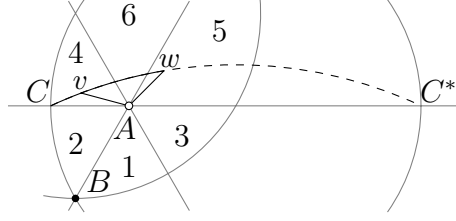


Figure 16: Deriving the boundary of the moduli space part in Ω_4 .

The polar equation is

$$r = \sqrt{\lambda_C^2 \sec^2 \theta + 1} - \lambda_C \sec \theta, \quad \theta \in [-\frac{1}{2}\pi, 0].$$

The spherical equation is

$$\xi = \frac{(\cos \theta, \sin \theta, -\lambda_C \sec \theta)}{\sqrt{\lambda_C^2 \sec^2 \theta + 1}}, \quad \theta \in [-\frac{1}{2}\pi, 0].$$

We may further calculate the boundary of the moduli space part in Ω_8 ($n = 3, 4$) or $\Omega_8 \cup \Omega_{14}$ ($n = 5$), in the B -projection. The coefficient

$$\lambda = \frac{1}{2}(d_{BM}^{-1} - d_{BM}) \cos \frac{1}{n}\pi = \frac{1}{2}(d_{AM}^{-1} - d_{AM}) \cos \frac{1}{3}\pi = \lambda_C.$$

The complex equation for the B -projection of γ_C is

$$4\lambda_C |z|^2 - (z + \bar{z})(|z|^2 - 1) = 0,$$

The cartesian equation is

$$2\lambda_C(x^2 + y^2) - x(x^2 + y^2 - 1) = 0,$$

The polar equation is

$$r = \sqrt{\lambda_C^2 \sec^2 \theta + 1} + \lambda_C \sec \theta, \quad \theta \in [-\pi, -\frac{1}{2}\pi].$$

The spherical equation is

$$\xi = \frac{(\cos \theta, \sin \theta, \lambda_C \sec \theta)}{\sqrt{\lambda_C^2 \sec^2 \theta + 1}}, \quad \theta \in [-\pi, -\frac{1}{2}\pi].$$

We note that the A -projection and the B -projection for γ_C are related by the transformation $(x, y) \mapsto (-x, y)$. Geometrically, this means that γ_C is symmetric with respect to the great circle of equal distance from A and B .

We use the same notation γ_C for the boundary curve in Ω_4 and in Ω_8 (or $\Omega_8 \cup \Omega_{14}$), because the two curves are actually the same one. Figure 17 gives the schematic reason for this claim. The curves in the two regions describe the extreme case that v lies on c (c_1 for Ω_4 and c_2 for Ω_8 (or $\Omega_8 \cup \Omega_{14}$)). Although w is an end of a_2 for the first region and an end of b_2 for the second region, the two versions of w and C, C^* are on the same great circle. Therefore the formulae for the curves are obtained by the same requirement that C, v, w, C^* are on the same great circle, irrespective to which w we choose.

In the polar equation for the A -projection of γ_C , the curve is in Ω_4 for $\theta \in [-\frac{1}{2}\pi, -\frac{1}{3}\pi]$, and in Ω_8 (or $\Omega_8 \cup \Omega_{14}$) for $\theta \in [-\frac{1}{3}\pi, 0]$. The two combine to yield the range $[-\frac{1}{2}\pi, 0]$ we gave earlier. Similar remark can be made for the polar equation for the B -projection of γ_C .

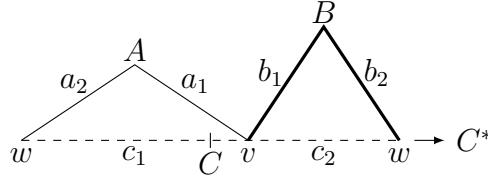


Figure 17: Moduli space parts in Ω_4 and Ω_8 (or $\Omega_8 \cup \Omega_{14}$) have the same boundary.

3 Picture of Moduli Space

By the discussion in Sections 1 and 2, the moduli space is the open subset of the sphere bounded by

- arcs $\Omega_3 \cap \Omega_9$ and $\Omega_7 \cap \Omega_9$;
- curve γ_A connecting two ends of $\Omega_3 \cap \Omega_5$, and inside Ω_5 ;
- curve γ_B connecting two ends of $\Omega_7 \cap \Omega_{13}$, and inside Ω_{13} (or $\Omega_{13} \cup \Omega_{19}$);
- curve γ_C connecting A to C to B , and inside Ω_4 and Ω_8 (or $\Omega_8 \cup \Omega_{14}$).

Figure 18 gives the perspective pictures of the three curves in the most convenient projections. Recall that the numbers 3, 4, 5 mean tetrahedron, octahedron, icosahedron. Moreover, the point B' is obtained by rotating B around A by $\frac{2}{3}\pi$, and A' is obtained by rotating A around B by $-\frac{2}{n}\pi$.

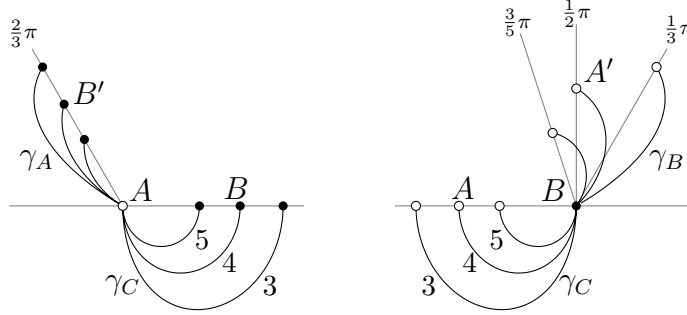


Figure 18: A -projection of γ_A, γ_C , and B -projection of γ_B, γ_C .

The most visually pleasing perspective picture of the moduli space is given by the M -projection in Figure 19. We also indicate the four congruent triangular regions $\Omega_1, \Omega_2, \Omega_3, \Omega_7$ contained in the moduli space. In the M -projection, $\Omega_1, \Omega_3, \Omega_7$ are visually congruent, and Ω_2 is the triangle outside Ω_1 . The following are some key points in the M -projection

$$A_M = -d_{AM}, \quad B_M = -d_{BM}i, \quad A'_M = d_{AM}, \quad B'_M = d_{BM}i.$$

To get the M -projection formulae for the three curves, we use the Möbius transform. The Möbius transform from the M -projection to the A -projection is easily determined by applying the transform to A, A^*, M

$$A_M \rightarrow A_A = 0, \quad A_M^* \rightarrow A_A^* = \infty, \quad M_M = 0 \rightarrow M_A.$$

We get

$$z_A = M_A \frac{A_M^*}{A_M} \cdot \frac{z_M - A_M}{z_M - A_M^*} = \frac{z_M + d_{AM}}{1 - d_{AM}z_M} e^{i\frac{1}{3}\pi}. \quad (3.1)$$

Substituting into the A -projection formulae of γ_A and γ_C , we get the M -projection formulae of γ_A and γ_C . Similarly, we get the M -projection formula of γ_B by

$$z_B = \frac{z_M + d_{BM}i}{1 + d_{BM}iz_M} e^{i(\frac{1}{2} - \frac{1}{n})\pi}. \quad (3.2)$$

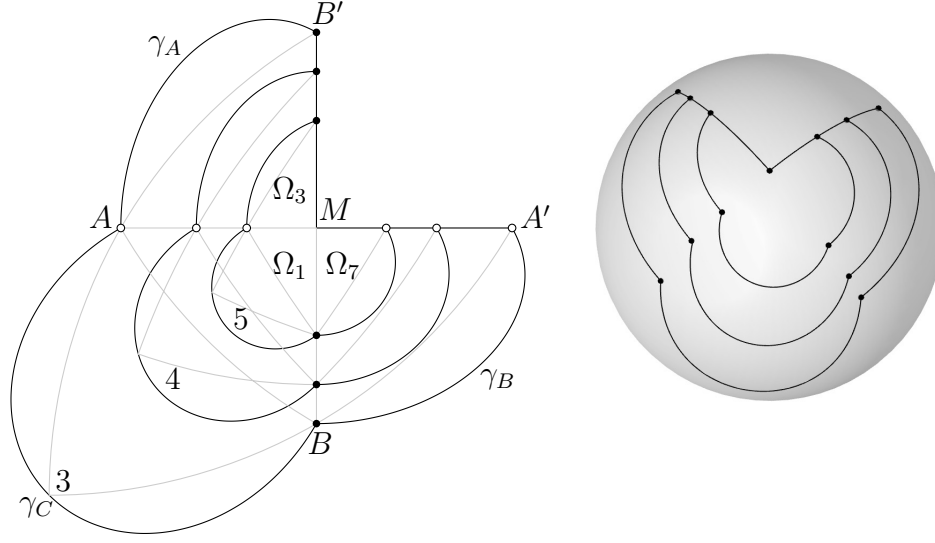


Figure 19: Moduli space of pentagonal subdivision in M -projection, and in sphere.

The first of Figure 19 gives the perspective pictures of the M -projections of $\gamma_A, \gamma_B, \gamma_C$.

The following are the cartesian forms of the three curves in the M -projection. For tetrahedron

$$\gamma_A: (x^2 + y^2)^2 + 2\sqrt{2}(x^2 + y^2)x - 8x^2 - 4y^2 - x + 1 = 0,$$

$$\gamma_B: (x^2 + y^2)^2 + 2\sqrt{2}(x^2 + y^2)y - 4x^2 - 8y^2 - y + 1 = 0,$$

$$\gamma_C: (x^2 + y^2 - 1)(x + y) - \sqrt{2}(x - y)^2 = 0.$$

For octahedron

$$\gamma_A: (x^2 + y^2)^2 - 10x^2 - 6y^2 + 1 = 0,$$

$$\gamma_B: (x^2 + y^2)^2 + 4(x^2 + y^2)y - 10x^2 - 14y^2 - 4y + 1 = 0,$$

$$\gamma_C: (x^2 + y^2 - 1)(x + \sqrt{2}y) - 2\sqrt{2}(x^2 + y^2) + 2xy = 0.$$

For icosahedron

$$\begin{aligned}
\gamma_A: & (x^2 + y^2)^2 - 2(\sqrt{5} - 1)(x^2 + y^2)x \\
& - 2(\sqrt{5} + 6)x^2 - 2(\sqrt{5} + 4)y^2 + 2(\sqrt{5} - 1)x + 1 = 0, \\
\gamma_B: & (x^2 + y^2)^2 + 2(\sqrt{5} + 1)(x^2 + y^2)y \\
& - 2(3\sqrt{5} + 8)x^2 - 2(3\sqrt{5} + 10)y^2 - 2(\sqrt{5} + 1)y + 1 = 0, \\
\gamma_C: & (x^2 + y^2 - 1)(2x + (\sqrt{5} + 1)y) \\
& - 2(\sqrt{5} + 3)(x^2 + y^2) + 2(\sqrt{5} - 1)xy = 0.
\end{aligned}$$

Using (2.1) and (2.2), the polar forms of the M -projections of the curves are given by ($R > 0$ and $1 > r > 0$)

$$r^{-1} - r = 2R, \quad r = \sqrt{R^2 + 1} - R,$$

and the spherical forms of the curves are given by

$$\xi = \frac{(\cos \theta, \sin \theta, -R)}{\sqrt{R^2 + 1}}.$$

The function R for the M -projection is explicitly given below

$$\begin{aligned}
R_A &= \begin{cases} \frac{\frac{1}{\sqrt{2}} \cos \theta + \frac{1}{\sqrt{2}} \sqrt{1 + 3 \cos^2 \theta}}{\sqrt{1 + \cos^2 \theta}}, & n = 3, \\ \sqrt{1 + \cos^2 \theta}, & n = 4, \\ \frac{\frac{1}{2}(1 - \sqrt{5}) \cos \theta + \frac{1}{\sqrt{2}} \sqrt{3 + \sqrt{5} + (5 - \sqrt{5}) \cos^2 \theta}}{\sqrt{1 + \cos^2 \theta}}, & n = 5; \end{cases} \\
R_B &= \begin{cases} \frac{\frac{1}{\sqrt{2}} \sin \theta + \frac{1}{\sqrt{2}} \sqrt{1 + 3 \sin^2 \theta}}{\sin \theta + \sqrt{2} \sqrt{1 + \sin^2 \theta}}, & n = 3, \\ \sin \theta + \sqrt{2} \sqrt{1 + \sin^2 \theta}, & n = 4, \\ \frac{\frac{1}{2}(1 + \sqrt{5}) \sin \theta + \frac{1}{\sqrt{2}} \sqrt{7 + 3\sqrt{5} + (5 + \sqrt{5}) \sin^2 \theta}}{\sin \theta + \sqrt{2} \sqrt{1 + \sin^2 \theta}}, & n = 5; \end{cases} \\
R_C &= \begin{cases} \frac{2 \cos \theta \sin \theta - 1}{\sqrt{2}(\cos \theta + \sin \theta)}, & n = 3, \\ \frac{\cos \theta \sin \theta - \sqrt{2}}{\cos \theta + \sqrt{2} \sin \theta}, & n = 4, \\ \frac{(\sqrt{5} - 1)(\cos \theta \sin \theta - \sqrt{5} - 2)}{2 \cos \theta + (\sqrt{5} + 1) \sin \theta}, & n = 5. \end{cases}
\end{aligned}$$

The range for the angle θ is $[\frac{1}{2}\pi, \pi]$ for γ_A , $[\frac{3}{2}\pi, 2\pi]$ for γ_B , and $[\pi, \frac{3}{2}\pi]$ for γ_C .

Finally, we remark that for γ_A and γ_B , R is given by another quadratic equation

$$R^2 - 2KR - L = 0, \quad R = \sqrt{K^2 + L} + K,$$

where K and L are given below.

	3	4	5
K_A	$\frac{1}{\sqrt{2}} \cos \theta$	0	$-\frac{1}{2}(\sqrt{5} - 1) \cos \theta$
L_A	$\cos^2 \theta + \frac{1}{2}$	$\cos^2 \theta + 1$	$\cos^2 \theta + \frac{1}{2}(\sqrt{5} + 3)$
K_B	$\frac{1}{\sqrt{2}} \sin \theta$	$\sin \theta$	$\frac{1}{2}(\sqrt{5} + 1) \sin \theta$
L_B	$\sin^2 \theta + \frac{1}{2}$	$\sin^2 \theta + 2$	$\sin^2 \theta + \frac{1}{2}(3\sqrt{5} + 7)$

4 Features of Moduli Space

4.1 Companion

The *companion* of pentagonal subdivision is introduced at the end of [11, Section 3.1]. In Figure 20, the companion of the pentagon with anchor point V is the pentagon with anchor point V' . We see that V' is the reflection of V with respect to the arc BB' in Figure 1. For a pentagonal subdivision to have the companion, therefore, the necessary and sufficient condition is both V and V' are inside the moduli space.

In the M -projection, we have the formulae for R_B and R_C . We may verify that $R_B(2\pi - \rho) \geq R_C(\pi + \rho)$ for $\rho \in [0, \frac{1}{2}\pi]$. This means that the reflection γ'_B of γ_B with respect to the arc BB' lies inside the moduli space. Therefore a pentagonal subdivision has companion, if and only if the anchor point V lies in the region bounded by the arc AA' , the curve γ_B , and the curve γ'_B .

In the M -projection, since the cartesian form of γ_B is even in x , we know γ'_B has the same algebraic formula as γ_B . In other words, the region for the companion to exist is bounded by the x -axis, and the $y \leq 0$ part of the algebraic formula for γ_B .

We remark that a pentagonal subdivision is the companion of itself, if and only if $V = V'$. This means exactly V lies on BM .

4.2 Location of Boundary

In Figures 3, 7, 9, 10, we divide the sphere into triangular regions. We know the locations of $\gamma_A, \gamma_B, \gamma_C$ in terms of these regions. However, the regions do

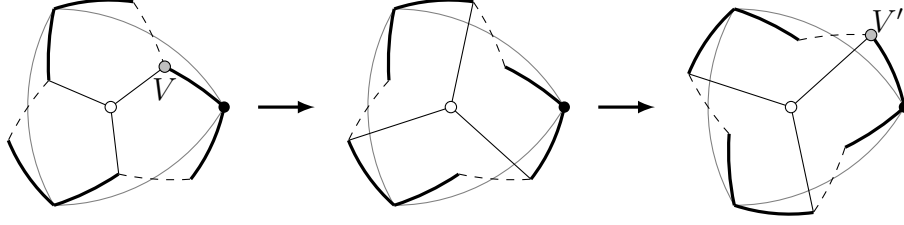


Figure 20: The companion of V is V' .

not have the same size. The smallest regions are $\Omega_1, \Omega_2, \Omega_3, \Omega_4, \Omega_7, \Omega_8$, with area $(\frac{1}{n} - \frac{1}{6})\pi$. We further divide the sphere into triangular regions of the same size or even smaller, and then find more precise locations of $\gamma_A, \gamma_B, \gamma_C$ in terms of these smaller regions.

In the first of Figure 21, we have the A -projection of one regular triangular face of the tetrahedron. We have the regions $\Omega_1, \Omega_2, \Omega_3, \Omega_4$ as before. Let B', M' be the rotations of B, M by $\frac{2}{3}\pi$. Let B'' be the rotation of B by $\frac{4}{3}\pi$. Let AX be the ray at angle $\frac{5}{6}\pi$, intersecting $B'B''$ at X . Then $\triangle AB'X$ is part of Ω_5 .

We know γ_A lies in Ω_5 , and between rays AB' and AX . For any point $@$ on $B'X$, we get $\underline{@}$ by rotating $-\frac{2}{3}\pi$ around A . Then $\underline{@}$ lies on BM , and the arc $B@$ lies inside $\triangle BB'M'$. This implies that $A\underline{@}$ intersects $B@$. Therefore $B'X$ is outside the moduli space. Combined with the fact that γ_A connects A and B' , AB' is in the moduli space, and AX is not in the moduli space, we conclude that γ_A is inside $\triangle AB'X$.

We also draw γ_C in the first of Figure 21. We know the Ω_4 -part of γ_C is between the ray AC and the ray AY at angle $\frac{3}{2}\pi$. The point Y is the intersection of $M'C$ and the ray AY . Then the picture shows that any point \odot on CY is not inside the moduli space. Combined with the fact that the Ω_4 -part of γ_C connects A and C , AC is in the moduli space, and AY is not in the moduli space, we conclude that the Ω_4 -part of γ_C is inside $\triangle ACY$.

The A -projections for the octahedron and icosahedron are similar to the first of Figure 21, and we have the similar $\triangle AB'X$ and $\triangle ACY$ for $n = 4, 5$. Since the argument above actually does not use the tetrahedron, we find γ_A is inside $\triangle AB'X$, and the Ω_4 -part of γ_C is inside $\triangle ACY$, also for $n = 4, 5$.

For the location of γ_B and the remaining part of γ_C , we use the B -projection. For the tetrahedron ($n = 3$), the picture is the the same as the horizontal flip of the A -projection (the first of Figure 21), with A and B exchanged. In fact, γ_A and the Ω_4 -part of γ_C are also transformed to γ_B

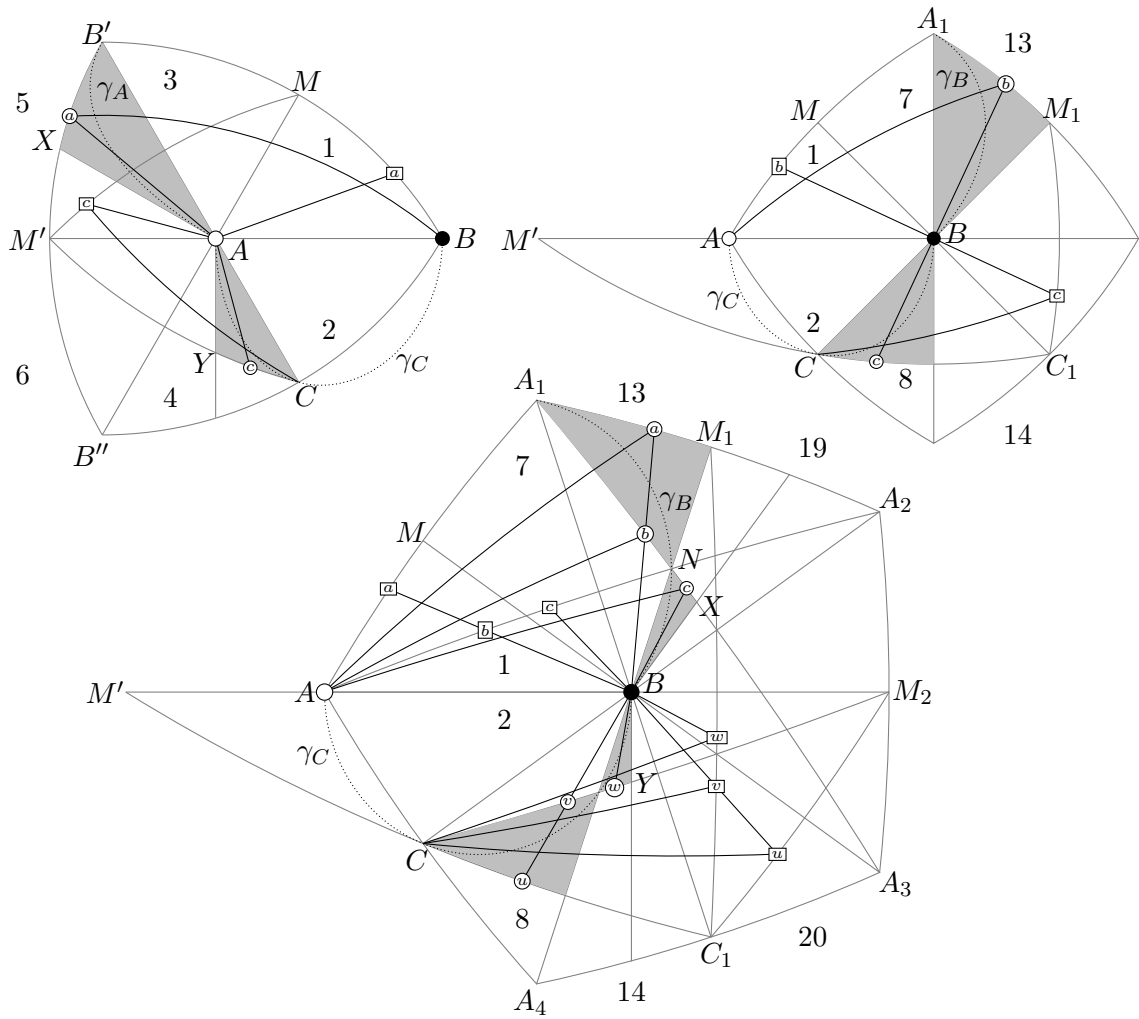


Figure 21: Locations of the boundary curves.

and the Ω_8 -part of γ_C in this way. Then we get the corresponding triangles containing γ_B and the Ω_8 -part of γ_C .

The second of Figure 21 is the B -projection for the octahedron. Let A_1, M_1 be the rotations of A, M around B by $-\frac{1}{2}\pi$ (A_1 is A' in Figure 18). Let C_1 be the rotation of C by $\frac{1}{2}\pi$. Then A_1M_1 cuts a triangle from Ω_{19} , and CC_1 cuts a triangle from Ω_8 . Both triangles are indicated by gray shade.

We know γ_B connects B and A_1 , and BM_1 is not in the moduli space. The picture shows that any point \textcircled{D} on A_1M_1 is not inside the moduli space. Therefore γ_B is inside $\triangle A_1BM_1$. Similar argument shows that the Ω_8 -part of γ_C lies in the other shaded triangle. We also note that M', C, C_1 lies in the same great circle. Therefore the whole $M'C_1$ is outside γ_C . Since γ_C passes C , we conclude that $M'C_1$ is tangential to γ_C .

The third of Figure 21 is the B -projection for the icosahedron. Let A_k, M_k be the rotations of A, M by $-\frac{2k}{5}\pi$. Let C_1 be the rotation of C by $\frac{2}{5}\pi$. Let BX and BY be the rays at angles $\frac{3}{10}\pi$ and $\frac{3}{2}\pi$. We see BX intersects A_1A_3 at X , and BY intersects CM_2 at Y .

The arcs AA_2, A_1A_3, BM_1 intersect at a point N . It is easy to verify that N is a point on γ_B . By Lemma 2, this implies BN is inside the moduli space, and NM_1 is outside the moduli space. We also know BX is outside the moduli space. The picture shows that A_1N is inside the moduli space, and A_1M_1, NX are outside the moduli space. Then we conclude γ_B is inside $\triangle A_1M_1N \cup \triangle BNX$.

The arcs CM_2, BA_4 intersect at a point, that we can easily verify to be on γ_C . We have two shaded triangles bounded by BA_4, BY, CC_1, CM_2 . By an argument similar to γ_B , we know γ_C is inside the union of the two shaded triangles. We also note that, similar to the octahedron, M', C, C_1 are on the same great circle. This implies $M'C_1$ is tangential to γ_C at C .

4.3 Upper Bound of Edge Length

Theorem 3. *The suprema of a, b, c in the pentagonal subdivision tiling are given by Table 3.*

The decimal value 0.6259072384π means

$$0.6259072383\pi < \sup a < 0.6259072384\pi.$$

In fact, we obtain the precise value

$$\sup a = 2 \arctan(\sqrt{R_B(\theta_{AB})^2 + 1} - R_B(\theta_{AB})),$$

	$n = 3$	$n = 4$	$n = 5$
sup a	0.6259072384π	0.4171042591π	0.2569674158π
sup b	0.6259072384π	$\frac{1}{2}\pi$	$\arccos \frac{1}{\sqrt{5}}$
sup c	π	0.6882086654π	0.4357713623π

Table 3: The suprema of the edges in the pentagonal subdivision tiling.

where $R_B(\theta)$ is given by (4.1), and the precise value of $\tan \theta_{AB}$ is given after (4.1), in terms of square and cube roots.

The same remark applies to the other decimal values, and we also obtain the precise values.

The supremum of a is the biggest of the maximal distances from A to $\gamma_A, \gamma_B, \gamma_C$. Here we have the supremum instead of the maximum because the moduli space is an open subset.

In the A -projection, the bigger Euclidean distance from A (this is r in (2.7) and (2.8)) is equivalent to the bigger spherical distance from A . We also know the polar versions (2.7) and (2.8) of γ_A and γ_C are strictly monotone with respect to the angle ϕ . Moreover, the whole γ_C is given by the same formulae (2.7) and (2.8), and the whole range is $\phi \in [\alpha, \alpha + \frac{1}{2}\pi]$. Then we find R and r are strictly monotone in ϕ on the whole range. Therefore we get (see Figure 18)

$$d_A(A, \gamma_A) = |AB'|_A = d_{AB}, \quad d_A(A, \gamma_C) = |AB|_A = d_{AB}.$$

Here $d_A(A, \gamma)$ is the Euclidean distance from A to curve γ in the A -projection. By applying the same reason to the B -projection, we get

$$d_B(B, \gamma_B) = |BA'|_B = d_{AB}, \quad d_B(B, \gamma_C) = |BA|_B = d_{AB}.$$

In Figure 21, we always have $d_A(A, \gamma_B) \geq |AA_1|_A = |AA'|_A > d_{AB}$. We also have $d_B(B, \gamma_A) \geq |BB'|_B > d_{AB}$. Therefore

$$\sup a = d_{\mathbb{S}}(A, \gamma_B), \quad \sup b = d_{\mathbb{S}}(B, \gamma_A).$$

Here the subscript \mathbb{S} indicates the spherical distance.

For $n = 4$, we have (the spherical distance) $|BP|_{\mathbb{S}} = |BB'|_{\mathbb{S}} = \frac{1}{2}\pi$ for any P on $B'M'$. For $n = 5$, we know $|BP|_{\mathbb{S}}$ is strictly decreasing as P moves from B' to M' along $B'M'$. Therefore

$$\sup b = |BB'|_{\mathbb{S}} = \begin{cases} \frac{1}{2}\pi, & n = 4, \\ \arccos \frac{1}{\sqrt{5}}, & n = 5. \end{cases}$$

By the symmetry, we have $\sup a = \sup b$ for $n = 3$. Therefore for the bounds of a and b , it remains to calculate $d_{\mathbb{S}}(A, \gamma_B)$.

As to the supremum of c , we note that $\sup \frac{1}{2}c$ is the biggest of the maximal distances from M to $\gamma_A, \gamma_B, \gamma_C$. The three maximal distances can be calculated by the M -projections of the three curves. This corresponds to minimizing R_A, R_B, R_C given at the end of Section 3.

For $\min R_C$, we recall the range $\theta \in [\pi, \frac{3}{2}\pi]$ for γ_C . For $n = 3$, the solution θ_{MC} of $R'_C(\theta) = 0$ satisfies

$$\tan \theta_{MC} = 1.$$

Correspondingly, we have

$$\theta_{MC} = \frac{5}{4}\pi, \quad R_C(\theta_{MC}) = 0.$$

By $R_C(\theta_{MC}) < R_C(\pi) = R_C(\frac{3}{2}\pi) = \frac{1}{\sqrt{2}}$, we get

$$\min R_C = R_C(\theta_{MC}).$$

Correspondingly, we have

$$\begin{aligned} \max r_C &= r_C(\theta_{MC}) = \sqrt{R_C(\theta_{MC})^2 + 1} - R_C(\theta_{MC}) = 1, \\ d_{\mathbb{S}}(M, \gamma_C) &= 2 \arctan \max r_C = \frac{1}{2}\pi. \end{aligned}$$

For $n = 4$, the solution θ_{MC} of $R'_C(\theta) = 0$ satisfies

$$\tan \theta_{MC} = \frac{1}{6\sqrt{2}}((\sqrt{17} - 5)T^{\frac{1}{3}} + (\sqrt{17} + 5)T^{-\frac{1}{3}} + 2), \quad T = \frac{1}{4}(\sqrt{17} + 1).$$

The corresponding

$$\begin{aligned} R_C(\theta_{MC}) &= \frac{\sqrt{17}}{18\sqrt{3}} \left((\sqrt{17} - 1)T^{\frac{1}{3}} - (\sqrt{17} + 1)T^{-\frac{1}{3}} + \frac{10}{\sqrt{17}} \right) \\ &\quad \sqrt{(\sqrt{17} + 1)T^{\frac{1}{3}} + (\sqrt{17} - 1)T^{-\frac{1}{3}} + 5} \\ &= \frac{\sqrt{17}}{9\sqrt{3}} \left(2T^{-\frac{2}{3}} - 2T^{\frac{2}{3}} + \frac{5}{\sqrt{17}} \right) \sqrt{4T^{\frac{4}{3}} + 4T^{-\frac{4}{3}} + 5} \\ &= 0.53308. \end{aligned}$$

We may verify $R_C(\theta_{MC}) < R_C(\pi) = R_C(\frac{3}{2}\pi)$. This implies $\min R_C = R_C(\theta_{MC})$.

For $n = 5$, the solution θ_{MC} of $R'_C(\theta) = 0$ satisfies

$$\begin{aligned}\tan \theta_{MC} &= \frac{1}{6\sqrt{5}\sqrt{1+3\sqrt{5}}} \left((-\sqrt{3}(11+7\sqrt{5})\sqrt{\sqrt{5}-2} + \sqrt{14}\sqrt{7+9\sqrt{5}})T^{\frac{1}{3}} \right. \\ &\quad \left. + (\sqrt{3}(11+7\sqrt{5})\sqrt{\sqrt{5}-2} + \sqrt{14}\sqrt{7+9\sqrt{5}})T^{-\frac{1}{3}} \right. \\ &\quad \left. + (3+\sqrt{5})\sqrt{1+3\sqrt{5}} \right), \\ T &= \frac{3\sqrt{3}(3-\sqrt{5})\sqrt{2+\sqrt{5}} + \sqrt{70}\sqrt{7+9\sqrt{5}}}{2(1+3\sqrt{5})^{\frac{3}{2}}}.\end{aligned}$$

The corresponding

$$\begin{aligned}R_C(\theta_{MC}) &= \frac{1}{60\sqrt{30}\sqrt{4+\sqrt{5}(1+3\sqrt{5})^{\frac{1}{4}}}} \\ &\quad \left((\sqrt{3}(17+21\sqrt{5})\sqrt{3+\sqrt{5}} - \sqrt{140}\sqrt{19-\sqrt{5}})T^{\frac{1}{3}} \right. \\ &\quad \left. + (-\sqrt{3}(17+21\sqrt{5})\sqrt{3+\sqrt{5}} - \sqrt{140}\sqrt{19-\sqrt{5}})T^{-\frac{1}{3}} \right. \\ &\quad \left. + 2(37-\sqrt{5})\sqrt{4+\sqrt{5}} \right) \\ &\quad \left(4(\sqrt{3}(\sqrt{5}-1)\sqrt{\sqrt{5}-2} + \sqrt{14}\sqrt{7+9\sqrt{5}})T^{\frac{1}{3}} \right. \\ &\quad \left. + 4(-\sqrt{3}(\sqrt{5}-1)\sqrt{\sqrt{5}-2} + \sqrt{14}\sqrt{7+9\sqrt{5}})T^{-\frac{1}{3}} \right. \\ &\quad \left. + (27+\sqrt{5})\sqrt{1+3\sqrt{5}} \right)^{\frac{1}{2}} \\ &= 1.22527.\end{aligned}$$

We may also verify $R_C(\theta_{MC}) < R_C(\pi) = R_C(\frac{3}{2}\pi)$. This implies $\min R_C = R_C(\theta_{MC})$.

Similarly, by the formulae for R_A, R_B , we may easily find

$$\min R_A = \min R_B = \begin{cases} \frac{1}{\sqrt{3}} = 0.57735, & n = 3, \\ 1, & n = 4, \\ \frac{1}{2}(\sqrt{5} + 1) = 1.61803, & n = 5. \end{cases}$$

We always have $\min R_A = \min R_B > \min R_C$. This means

$$\max r_A = \max r_B < \max r_C = r_C(\theta_{MC}) = \sqrt{R_C(\theta_{MC})^2 + 1} - R_C(\theta_{MC}).$$

Then we have

$$\sup c = 2d_S(M, \gamma_C) = 4 \arctan r_C(\theta_{MC}) = \begin{cases} \pi, & n = 3, \\ 0.6882086653\pi, & n = 4, \\ 0.4357713622\pi, & n = 5. \end{cases}$$

The value 0.6882086653π means $0.6882086653\pi < \sup c < 0.6882086654\pi$. We add $10^{-10}\pi$ to get the values in Table 3.

Now we calculate $\sup a = d_S(A, \gamma_B)$ in the similar way. First, we use the Möbius transform to find the polar formula for the A -projection of γ_B . It is given by $r_B = \sqrt{R_B^2 + 1} - R_B$ with

$$R_B = \begin{cases} \frac{\sqrt{3} - 8 \cos \theta \sin \theta}{2\sqrt{2}(\sqrt{3} \cos \theta + \sin \theta)}, & n = 3, \\ \frac{\sqrt{3} - 2 \cos \theta \sin \theta}{\sqrt{2}(\sqrt{3} \cos \theta + \sin \theta)}, & n = 4, \\ \frac{\sqrt{3}(3\sqrt{5} + 7) - 8 \cos \theta \sin \theta}{2(3 - \sqrt{5})(\sqrt{3} \cos \theta + \sin \theta)}, & n = 5. \end{cases} \quad (4.1)$$

The range is $\theta \in [0, \frac{1}{3}\pi]$. For $n = 3$, the solution θ_{AB} of $R'_B(\theta) = 0$ satisfies

$$\tan \theta_{AB} = \frac{1}{77\sqrt{3}}((15\sqrt{3} + \sqrt{451})T^{\frac{1}{3}} + 7(-15\sqrt{3} + \sqrt{451})T^{-\frac{1}{3}} + 7),$$

$$T = 6\sqrt{3} + \sqrt{451}.$$

For $n = 4$, we have

$$\tan \theta_{AB} = \frac{1}{25\sqrt{3}}((6\sqrt{3} + \sqrt{38})T^{\frac{1}{3}} + 5(-6\sqrt{3} + \sqrt{38})T^{-\frac{1}{3}} + 5),$$

$$T = 3\sqrt{3} + 2\sqrt{38}.$$

For $n = 5$, we have

$$\tan \theta_{AB} = \frac{1}{218\sqrt{6}(7+4\sqrt{5})} \left((\sqrt{2}(5\sqrt{5} - 4)\sqrt{501 + 127\sqrt{5}} + 3\sqrt{3}(31 + 43\sqrt{5}))T^{\frac{1}{3}} \right. \\ \left. + (27 + 11\sqrt{5})(\sqrt{2}(5\sqrt{5} - 4)\sqrt{501 + 127\sqrt{5}} - 3\sqrt{3}(31 + 43\sqrt{5}))T^{-\frac{1}{3}} \right) \\ + \frac{1}{109\sqrt{3}}(17 + 6\sqrt{5}),$$

$$T = (3\sqrt{5} + 7)(3\sqrt{6} + \sqrt{501 + 127\sqrt{5}}).$$

We verify the corresponding θ_{AB} is always in $[0, \frac{1}{3}\pi]$. Then we verify $R_B(\theta_{AB}) < R_B(\frac{1}{3}\pi) < R_B(0)$ always holds. Then we conclude

$$\sup a = d_{\mathbb{S}}(A, \gamma_B) = 2 \arctan r_B(\theta_{AB}) = \begin{cases} 0.6259072383\pi, & n = 3, \\ 0.4171042590\pi, & n = 4, \\ 0.2569674157\pi, & n = 5. \end{cases}$$

We add $10^{-10}\pi$ to get the values in Table 3.

4.4 Reduction

The pentagon in the pentagonal subdivision of a Platonic solid has three edge lengths a, b, c . The edge lengths are generally not equal, and we get a tiling of the sphere by congruent pentagons with the edge length combination a^2b^2c . When some edge lengths become equal, then the tiling has a different edge length combination.

For example, if $a = b$, then the edge length combination a^2b^2c is reduced to a^4b (with $a = b$ labeled as the new a , and c labeled as the new b), and we get a tiling of the sphere by congruent *almost equilateral* pentagons. The reduction means $|AV|_{\mathbb{S}} = |BV|_{\mathbb{S}}$. All the points of equal distance from A and B form a great circle. By $\tan \frac{1}{2}|AV|_{\mathbb{S}} = |z_A|$ and $\tan \frac{1}{2}|BV|_{\mathbb{S}} = |z_B|$, the equality $|AV|_{\mathbb{S}} = |BV|_{\mathbb{S}}$ becomes $|z_A| = |z_B|$. Let $z = z_M$ be the complex coordinate of V in the M -projection. Then we substitute (3.1) and (3.2) into $|z_A| = |z_B|$, and get the equation of the circle

$$n = 3: x - y = 0,$$

$$n = 4: x^2 + y^2 + 2(\sqrt{3} + 2)(\sqrt{2}x - \sqrt{3}y) - 1 = 0,$$

$$n = 5: x^2 + y^2 - 2((\sqrt{5} - 11)\mu - \sqrt{5})x - 2((5\sqrt{5} + 3)\mu + 3)y - 1 = 0,$$

$$\mu = \frac{1}{58}\sqrt{195 - 6\sqrt{5}}.$$

For $n = 3$, the circle is actually the diagonal line. For $n = 4$, the circle has center $(-\sqrt{2}(2 + \sqrt{3}), \sqrt{3}(2 + \sqrt{3}))$ and radius $2\sqrt{9 + 5\sqrt{3}}$. For $n = 5$, the center is $((\sqrt{5} - 11)\mu - \sqrt{5}, (5\sqrt{5} + 3)\mu + 3)$, and the radius is $\sqrt{4(13\sqrt{5} + 2)\mu + 30}$.

The circle is also the intersection of the sphere with a plane. The following

is the equation of this plane

$$n = 3: \xi_1 - \xi_2 = 0,$$

$$n = 4: \sqrt{2}\xi_1 - \sqrt{3}\xi_2 - (\sqrt{3} - 2)\xi_3 = 0,$$

$$n = 5: 2 \cdot 5^{\frac{1}{4}}\xi_1 - \sqrt{6}\sqrt{\sqrt{5} + 1}\xi_2 + ((\sqrt{5} + 3)5^{\frac{1}{4}} - \frac{\sqrt{3}}{\sqrt{2}}(\sqrt{5} + 1)^{\frac{3}{4}})\xi_3 = 0.$$

If $a = c$ or $b = c$, then we get a tiling of the sphere by congruent pentagons with the edge length combination a^3b^2 . The reduction $a = c$ is the same as $a = 2c_1$, or $|AV|_S = 2|MV|_S$. By $\tan \frac{1}{2}|AV|_S = |z_A|$ and $\tan \frac{1}{2}|MV|_S = |z_M| = |z|$, the equality $|AV|_S = 2|MV|_S$ becomes

$$|z_A| = \frac{2|z|}{1 - |z|^2}.$$

Applying (3.1), we get the equation in the M -projection

$$n = 3: (x^2 + y^2)^2 + \sqrt{2}(\sqrt{3} - 1)(x^2 + y^2)x - 3\sqrt{3}(\sqrt{3} - 1)(x^2 + y^2) + \sqrt{2}(\sqrt{3} - 1)x - \sqrt{3} + 2 = 0,$$

$$n = 4: (x^2 + y^2)^2 + 2(\sqrt{3} - \sqrt{2})(x^2 + y^2)x - 6\sqrt{3}(\sqrt{3} - \sqrt{2})(x^2 + y^2) + 2(\sqrt{3} - \sqrt{2})x - 2\sqrt{6} + 5 = 0,$$

$$n = 5: (x^2 + y^2)^2 + (\sqrt{5} - \sqrt{3})(\sqrt{3} - 1)(x^2 + y^2)x + 3(2\sqrt{15} - 3\sqrt{5} + 4\sqrt{3} - 9)(x^2 + y^2) + (\sqrt{5} - \sqrt{3})(\sqrt{3} - 1)x - 2\sqrt{15} + 3\sqrt{5} - 4\sqrt{3} + 8 = 0.$$

It is very easy to convert the cartesian form to the polar form

$$n = 3: r^4 - 3\sqrt{3}(\sqrt{3} - 1)r^2 - \sqrt{3} + 2 + \sqrt{2}(\sqrt{3} - 1)r(r^2 + 1)\cos\theta = 0$$

$$n = 4: r^4 - 6\sqrt{3}(\sqrt{3} - \sqrt{2})r^2 - 2\sqrt{6} + 5 + 2(\sqrt{3} - \sqrt{2})r(r^2 + 1)\cos\theta = 0,$$

$$n = 5: r^4 + 3(2\sqrt{15} - 3\sqrt{5} + 4\sqrt{3} - 9)r^2 - 2\sqrt{15} + 3\sqrt{5} - 4\sqrt{3} + 8 + (\sqrt{5} - \sqrt{3})(\sqrt{3} - 1)r(r^2 + 1)\cos\theta = 0.$$

The curve is also the intersection of the sphere with a parabolic cylinder

$$n = 3: 2\sqrt{3}\xi_3^2 + \sqrt{2}\xi_1 + \xi_3 - \sqrt{3} = 0,$$

$$n = 4: 2\sqrt{3}\xi_3^2 + \xi_1 + \sqrt{2}\xi_3 - \sqrt{3} = 0,$$

$$n = 5: 4\sqrt{3}\xi_3^2 + (\sqrt{5} - 1)\xi_1 + (\sqrt{5} + 1)\xi_3 - 2\sqrt{3} = 0.$$

Similarly, the reduction $b = c$ means $|BV|_{\mathbb{S}} = 2|MV|_{\mathbb{S}}$, or

$$|z_B| = \frac{2|z|}{1 - |z|^2}.$$

Applying (3.2), we get the equation in the M -projection

$$\begin{aligned} n = 3: & (x^2 + y^2)^2 + \sqrt{2}(\sqrt{3} - 1)(x^2 + y^2)y - 3\sqrt{3}(\sqrt{3} - 1)(x^2 + y^2) \\ & + \sqrt{2}(\sqrt{3} - 1)y - \sqrt{3} + 2 = 0, \\ n = 4: & (x^2 + y^2)^2 + 2(\sqrt{2} - 1)(x^2 + y^2)y - 6\sqrt{2}(\sqrt{2} - 1)(x^2 + y^2) \\ & + 2(\sqrt{2} - 1)y - 2\sqrt{2} + 3 = 0, \\ n = 5: & (x^2 + y^2)^2 + (\sqrt{2}(\sqrt{5} + 1)^{\frac{1}{2}}5^{\frac{1}{4}} - \sqrt{5} - 1)(x^2 + y^2)x \\ & + 3\left(\frac{1}{\sqrt{2}}(\sqrt{5} + 1)^{\frac{3}{2}}5^{\frac{1}{4}} - \sqrt{5} - 5\right)(x^2 + y^2) \\ & + (\sqrt{2}(\sqrt{5} + 1)^{\frac{1}{2}}5^{\frac{1}{4}} - \sqrt{5} - 1)x \\ & - \frac{1}{\sqrt{2}}(\sqrt{5} + 1)^{\frac{3}{2}}5^{\frac{1}{4}} + \sqrt{5} + 4 = 0. \end{aligned}$$

It is also easy to get the polar form, or view the curve as the intersection of the sphere with a parabolic cylinder

$$\begin{aligned} n = 3: & 2\sqrt{3}\xi_3^2 + \sqrt{2}\xi_2 + \xi_3 - \sqrt{3} = 0, \\ n = 4: & 2\sqrt{2}\xi_3^2 + \xi_2 + \xi_3 - \sqrt{2} = 0, \\ n = 5: & 2\sqrt{2} \cdot 5^{\frac{1}{4}}\xi_3^2 + \sqrt{\sqrt{5} - 1}\xi_2 + \sqrt{\sqrt{5} + 1}\xi_3 - \sqrt{2} \cdot 5^{\frac{1}{4}} = 0. \end{aligned}$$

Figure 22 is the perspective picture of the reduced curves in the M -projection and in the sphere. From the picture, we notice that the curve $b = c$ is tangential to and is also below the boundary γ_A of the moduli space for $n = 4$. We confirmed this through Taylor expansion. The picture also suggests that each pentagonal subdivision has a unique equilateral pentagon (i.e., $a = b = c$). The uniqueness of the equilateral pentagonal subdivisions are rigorously verified in [1, 2].

4.5 Size of Moduli Space

In a stereographic projection, we consider the fan region between the origin and a curve $r = r(\theta)$, $\theta \in [\alpha, \beta]$. The corresponding region in the sphere has area

$$\int_{\alpha}^{\beta} \frac{2r^2 d\theta}{1 + r^2}.$$

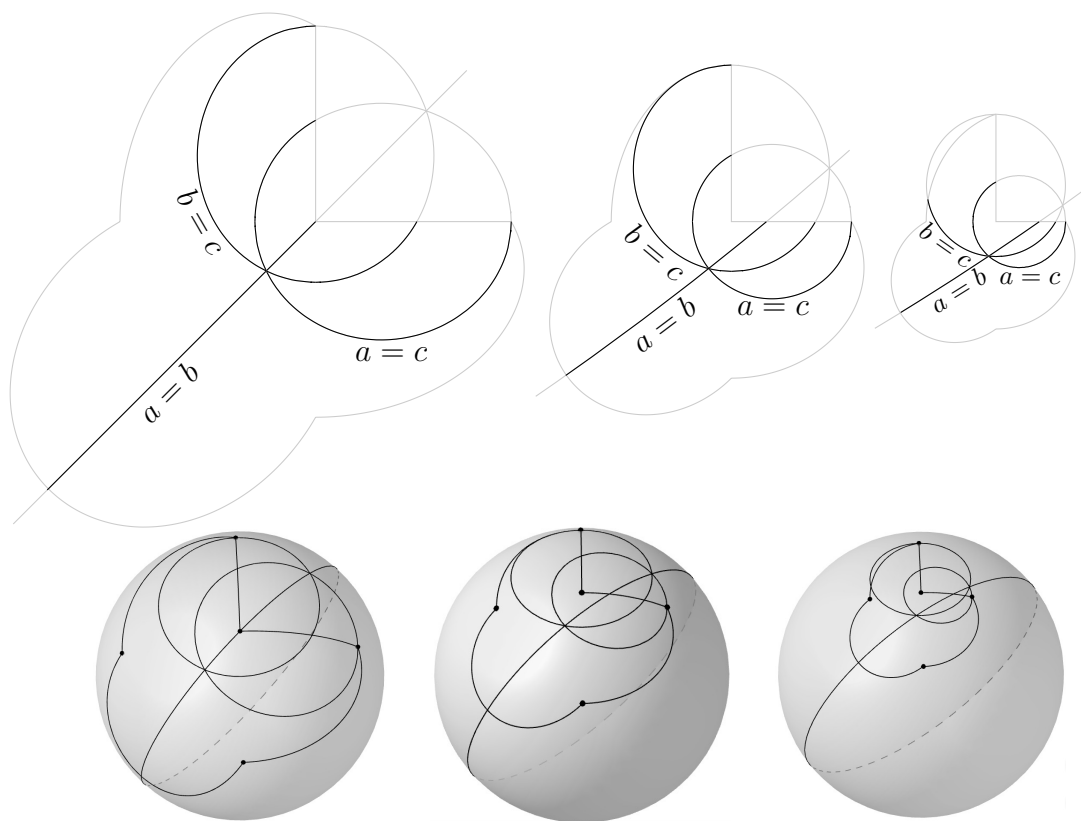


Figure 22: Reduction curves in the moduli space.

Then the area of the region given by (2.7) and (2.8) is ($\theta = \phi - \alpha$)

$$\int_{\alpha}^{\frac{1}{2}\pi} \frac{2r^2 d\theta}{1+r^2} = \int_{\alpha}^{\frac{1}{2}\pi} \left(1 - \frac{R}{\sqrt{R^2+1}}\right) d\theta = \frac{1}{2}\pi - \alpha - F\left(\frac{1}{2}\pi - \alpha, \lambda^{-1}i\right),$$

where $R = \lambda \sec \theta$, and

$$F(t, k) = \int_0^t \frac{dt}{\sqrt{1 - k^2 \sin^2 t}}$$

is the elliptic integral of the first kind.

We may apply the formula to the A -projection of γ_A to get the area of the moduli space part in Ω_5

$$A_5 = \frac{1}{6}\pi - F\left(\frac{1}{6}\pi, \lambda_A^{-1}i\right).$$

We may also apply the formula to the B -projection of γ_B to get the area of the moduli space part in Ω_{13} (for $n = 5$, the notation A_{13} also includes the moduli space part in Ω_{19})

$$A_{13} = \left(\frac{1}{2} - \frac{1}{n}\right)\pi - F\left(\left(\frac{1}{2} - \frac{1}{n}\right)\pi, \lambda_B^{-1}i\right).$$

We may use the same idea to get (for $n = 5$, the notation A_8 also includes the moduli space part in Ω_{14})

$$\begin{aligned} A_4 &= \frac{1}{6}\pi - F\left(\frac{1}{6}\pi, \lambda_C^{-1}i\right), \\ A_8 &= \left(\frac{1}{2} - \frac{1}{n}\right)\pi - F\left(\left(\frac{1}{2} - \frac{1}{n}\right)\pi, \lambda_C^{-1}i\right). \end{aligned}$$

We may also use the fact that γ_C has the same formula in Ω_4 and Ω_8 to get

$$A_2 + A_4 + A_8 = \frac{1}{2}\pi - F\left(\frac{1}{2}\pi, \lambda_C^{-1}i\right).$$

Finally, the moduli space contains the whole triangles $\Omega_1, \Omega_2, \Omega_3, \Omega_7$, which are congruent triangles and have the same area

$$A_1 = A_2 = A_3 = A_7 = \frac{1}{6N}4\pi, \quad N = 4, 8, 20 \text{ for } n = 3, 4, 5.$$

The whole area of the moduli space is

$$A_1 + A_2 + A_3 + A_4 + A_5 + A_7 + A_8 + A_{13} = \begin{cases} 0.8600517493\pi, & n = 3, \\ 0.4602931496\pi, & n = 4, \\ 0.1954959087\pi, & n = 5. \end{cases}$$

References

- [1] Y. Akama, M. Yan. On deformed dodecahedron tiling. *Australas. J. Comb.*, 65(1):1–14, 2023.
- [2] Y. Akama, E. Wang, M. Yan. Tilings of sphere by congruent pentagons III: edge combination a^5 . *Adv. Math.*, 394:107881, 2022.
- [3] H. M. Cheung, H. P. Luk, M. Yan. Tilings of the sphere by congruent pentagons IV: edge combination a^4b . preprint, arXiv:2307.11453, 2023.
- [4] H. M. Cheung, H. P. Luk, M. Yan. Tilings of the sphere by congruent quadrilaterals or triangles. preprint, arXiv:2204.02736, 2022.
- [5] H. H. Gao, N. Shi, M. Yan. Spherical tiling by 12 congruent pentagons. *J. Combinatorial Theory Ser. A*, 120(4):744–776, 2013.
- [6] Y. Liao, E. Wang. Tilings of the sphere by congruent quadrilaterals II: edge Combination a^3b with rational angles. *Nagoya Math. J.*, 253:128–163, 2024.
- [7] Y. Liao, E. Wang, P. Qian, Y. Xu. Tilings of the Sphere by Congruent Quadrilaterals I: Edge Combination a^2bc . *Chin. Ann. Math. Ser. B*, 45(5):1–34, 2024.
- [8] Y. Liao, E. Wang, P. Qian, Y. Xu. Tilings of the sphere by congruent quadrilaterals III: Edge Combination a^3b with general angles. *Forum Math.*, <https://doi.org/10.1515/forum-2023-0209>, 2024.
- [9] D. M. Y. Sommerville. Division of space by congruent triangles and tetrahedra. *Proc. Royal Soc. of Edinburgh*, 43:85–116, 1924.
- [10] Y. Ueno, Y. Agaoka. Classification of tilings of the 2-dimensional sphere by congruent triangles. *Hiroshima Math. J.*, 32(3):463–540, 2002.
- [11] E. Wang, M. Yan. Tilings of the sphere by congruent pentagons I: edge combinations a^2b^2c and a^3bc . *Adv. Math.*, 394:107866, 2022.
- [12] E. Wang, M. Yan. Tilings of the sphere by congruent pentagons II: edge combination a^3b^2 . *Adv. Math.*, 394:107867, 2022.